Final Report

MODEL FOR PREDICTION OF NOISE-INDUCE HEARING LOSS

April 2006

Principal Investigator and Project Director: *Roger P. Hamernik*, Ph.D.

Co-Investigators:

Wei Qiu, Ph.D.

Jun Ye, Ph.D.

AUDITORY RESEARCH LABORATORY

State University of New York at Plattsburgh

Plattsburgh, New York 12901

Sponsored by: NIOSH

Grant No.: 1-R01-OH007801-01A1

April, 2004 ~ March, 2006

Table of Contents

Abstract:

The primary goal of this research project was to demonstrate the feasibility of developing an optimal prediction model for noise-induced hearing loss (NIHL) using modern statistical learning methods. Three approaches were developed: (1) a multilayer perceptron network (MLP), (2) a radial basis function network (RBF) and (3) a support vector machine (SVM). The three statistical learning models were developed to predict noise-induced hearing loss (NIHL) from an archive of animal noise exposure data, which contains 900 chinchillas exposed to various noise environments..

There were basically two different kinds of noises that were used in these modeling studies: High level (peak>140dB) impulse noise transients, which typically occur in military environments, and low and medium level (peak<140dB) long term complex noise exposures, which usually occur in industrial environments. Both noise metrics and biological parameters were used as input variables to the prediction models. Since the prediction models consist of individual biological information, it should be possible to predict noise-induced hearing loss in an individual.

Two frequency specific prediction models were considered: One was a specific frequency model (SF model), the other was a wide band frequency model (WF model). In the SF model a prediction model was built for each specified frequency. In the WF prediction model contiguous frequency band information on either upper or lower side(s) of a specified frequency band were considered as additional input(s) for the models. Both SF and WF models were built and tested.

Two partition methods were used to stratify the data sets for training, validating and testing the prediction models. Partition method 1 considers all the data sets from the different noise types. The database is stratified according to exposure noises before sampling to make sure that the samples from different types of noise are allocated to both training and test data sets more or less equally. Partition method 2 neglects the fact that all available training data are collected under different exposure conditions. The samples from different groups are divided into disjoint sample sets of equal size randomly, without taking into account the different exposure groups. The prediction models using partition 1 and 2 were built and tested.

For long term complex noise exposures 10 noise metrics and 5 biological parameters were used as the inputs of the prediction model in the initial stage of the research project. Four prediction results at specific center frequencies were produced, i.e. noise-induced permanent threshold shift (PTS), inner hair cell (IHC) loss, outer hair cell (OHC) loss, and permanent change in cubic distortion product otoacoustic emission (ΔDPOAE). It was found that energy alone was not a sufficient metric to predict complex noise induced hearing hazard. Kurtosis is a complementary metric. With the kurtosis metric performance of the prediction models is improved as much as 66%. It was also found that some biological parameters, such as asymptotic threshold shift and pre-exposure DPOAE did not contribute much to increasing the prediction accuracy (in many cases these variables made the prediction results worse). In the final prediction model for complex noise exposures 6 noise metrics and one biological parameter were used as input variables to predict the NIHL in terms of PTS, IHC loss and OHC loss. It was found that the prediction models using the WF method would yield the best average prediction accuracy. Of the three prediction models, the RBF model produced the best performance. The percent prediction accuracy for IHC loss using the RBF model was 92%, OHC loss: 93% and PTS: 96%. The performance of the RBF models using partition method 1 and method 2 were not significantly different.

For impulse noise exposures parameters, such as peak, duration, number and rate, are important to the prediction of NIHL. The SVM model with the SF method was selected as the best prediction model. The percent prediction accuracy for IHC loss using the RBF model was 85%, OHC loss: 87% and PTS: 93%.

Abstract:

The primary goal of this research project was to demonstrate the feasibility of developing an optimal prediction model for noise-induced hearing loss (NIHL) using modern statistical learning methods. Three approaches were developed: (1) a multilayer perceptron network (MLP), (2) a radial basis function network (RBF) and (3) a support vector machine (SVM). The three statistical learning models were developed to predict noise-induced hearing loss (NIHL) from an archive of animal noise exposure data, which contains 900 chinchillas exposed to various noise environments..

There were basically two different kinds of noises that were used in these modeling studies: High level (peak>140dB) impulse noise transients, which typically occur in military environments, and low and medium level (peak<140dB) long term complex noise exposures, which usually occur in industrial environments. Both noise metrics and biological parameters were used as input variables to the prediction models. Since the prediction models consist of individual biological information, it should be possible to predict noise-induced hearing loss in an individual.

Two frequency specific prediction models were considered: One was a specific frequency model (SF model), the other was a wide band frequency model (WF model). In the SF model a prediction model was built for each specified frequency. In the WF prediction model contiguous frequency band information on either upper or lower side(s) of a specified frequency band were considered as additional input(s) for the models. Both SF and WF models were built and tested.

Two partition methods were used to stratify the data sets for training, validating and testing the prediction models. Partition method 1 considers all the data sets from the different noise types. The database is stratified according to exposure noises before sampling to make sure that the samples from different types of noise are allocated to both training and test data sets more or less equally. Partition method 2 neglects the fact that all available training data are collected under different exposure conditions. The samples from different groups are divided into disjoint sample sets of equal size randomly, without taking into account the different exposure groups. The prediction models using partition 1 and 2 were built and tested.

For long term complex noise exposures 10 noise metrics and 5 biological parameters were used as the inputs of the prediction model in the initial stage of the research project. Four prediction results at specific center frequencies were produced, i.e. noise-induced permanent threshold shift (PTS), inner hair cell (IHC) loss, outer hair cell (OHC) loss, and permanent change in cubic distortion product otoacoustic emission (ΔDPOAE). It was found that energy alone was not a sufficient metric to predict complex noise induced hearing hazard. Kurtosis is a complementary metric. With the kurtosis metric performance of the prediction models is improved as much as 66%. It was also found that some biological parameters, such as asymptotic threshold shift and pre-exposure DPOAE did not contribute much to increasing the prediction accuracy (in many cases these variables made the prediction results worse). In the final prediction model for complex noise exposures 6 noise metrics and one biological parameter were used as input variables to predict the NIHL in terms of PTS, IHC loss and OHC loss. It was found that the prediction models using the WF method would yield the best average prediction accuracy. Of the three prediction models, the RBF model produced the best performance. The percent prediction accuracy for IHC loss using the RBF model was 92%, OHC loss: 93% and PTS: 96%. The performance of the RBF models using partition method 1 and method 2 were not significantly different.

For impulse noise exposures parameters, such as peak, duration, number and rate, are important to the prediction of NIHL. The SVM model with the SF method was selected as the best prediction model. The percent prediction accuracy for IHC loss using the RBF model was 85%, OHC loss: 87% and PTS: 93%.

Highlight/Significant Findings:

1. Modern statistical algorithms, such as a radial basis function network (RBF) and a support vector machine (SVM) can be used to build robust prediction models for noise-induced hearing loss (NIHL). That is, to predict the consequences of a noise exposure for an individual in terms of permanent threshold shift, and sensory cell loss. The percent prediction accuracy for the various models was at least 85%. The best of the models could yield a prediction accuracy as high as 96%.
2. For long term complex noise exposures energy alone is not a sufficient metric to predict complex noise induced hearing loss. Kurtosis is a complementary metric. With the kurtosis metric performance of the prediction models is improved as much as 66%, a significant improvement.
3. Two partition methods were used to stratify the data sets for training, validating and testing the prediction models. It was found that the partition methods did not have a significant effect on the performance of the prediction models. The RBF and SVM models are effective and robust.
4. Two frequency specific prediction models were considered: One was a specific frequency model (SF model), the other was a wide band frequency model (WF model). In the SF model a prediction model was built for each specified frequency. In the WF prediction model contiguous frequency band information on either upper or lower side(s) of a specified frequency band were considered as additional input(s) for the models. It was found that the WF model did increase the prediction accuracy for complex noise exposures, while the SF model had a better performance for high level impulse noise exposures.

Translation of Findings:

In this research project we developed several modern statistical learning models to predict noise-induced effects on the peripheral auditory system in an animal model. The success of this initiative has demonstrated the feasibility of such an approach and has identified combinations of metrics that are important for predicting NIHL. Because of the similarity of the chinchilla and human response to noise the demonstration of the feasibility of such a modeling approach can form the basis for creating a predictive model applicable to humans and can lead to a new approach to creating a damage risk criteria. Since the prediction models consist of individual biological information, it should be possible to predict noise-induced hearing loss in an individual.

Outcomes/Relevance/Impact:

This research is the first of its kind to apply modern statistical prediction models to the problem of predicting noise-induced hearing loss in an individual. Two prediction models were developed for noise-induced hearing loss. The radial basis function (RBF) neural network model with wide-band frequency method was developed for long term complex noise exposures. The percent prediction accuracy for IHC loss using the RBF model was 92%, OHC loss: 93% and PTS: 96%. The support vector machine (SVM) model with the specific frequency method was built for high level impulse noise exposures. The percent prediction accuracy for IHC loss using the RBF model was 85%, OHC loss: 87% and PTS: 93%.

For long term complex noise exposures energy alone is not a sufficient metric to predict complex noise induced hearing hazard. Kurtosis is a complementary metric. With the kurtosis metric performance of the prediction models is improved as much as 66%, a significant improvement.

I. Introduction

This proposed two-year effort had a single "specific aim," which was to demonstrate the feasibility of developing an optimal prediction model for noise-induced hearing loss (NIHL) using modern statistical learning methods. Three approaches were developed: (1) a multilayer perceptron network (MLP), (2) a radial basis function network (RBFN) and (3) a support vector machine (SVM). The model with the best predictive performance is defined as optimal. The above models were created utilizing an extensive existing database to predict damage to the auditory system in the chinchilla from any noise environment that can be subjected to an analysis from which the standard as well as newer acoustic metrics can be extracted.

II. Background and Significance:

(1) Background: Since the beginning of the industrial revolution, NIHL has been and continues to be a public health concern and has been identified as such in the NOISH, National Occupational Research Agenda (NORA) document (1996). Over the last 50 years considerable data on NIHL has been amassed from epidemiological studies and animal-model research. Much of the former data has been embodied in the ISO-1999 (1990) document while a comprehensive synthesis of the latter, for use in guiding the development of improved damage risk criteria (DRC), has not been attempted. All of these studies ultimately have a single common objective: the prediction of noise-induced trauma from knowledge of the exposure conditions. This goal has remained elusive. The strengths and weaknesses of the ISO document, which is based on data collected in the 1950's and 60's, have been discussed (Johnson, 1994) and specific problem areas affecting all DRCs derived from epidemiological data highlighted (Ward, 1994). The ISO-1999 (1990) document is a revision of the 1975 version. It presents in statistical terms the relation between a noise exposure and a noise-induced hearing loss (NIHL) in people of various ages and having various exposure durations. The basic approach to this standard was formulated over 30 years ago and incorporates a demographic database acquired even earlier. In this widely used document (see e.g., Dobie, 1993; Bies and Hansen, 1990) all noise exposures are quantified by a single metric, that is, a time-integrated pressure-squared or energy metric incorporating a spectral weighting. Pure tone radiation and impulsive (impact) noises are assigned a 5 dB "correction." The energy approach to the standards document has been questioned by Bies and Hansen (1990) who showed that an alternate formulation (non-energy-based) is also consistent with the demographic database and by Kraak (1981) whose approach is consistent with that of Bies and Hansen. Similarly, there are many examples in the literature that demonstrate, on the basis of experimental evidence, the limitations of an energy metric (e.g., Lei et al., 1994). The ISO approach to an age correction has also been questioned on methodological grounds by Bies and Hansen (1990) and by Humes and Jesteadt (1991) and most recently on experimental grounds by Mills et al., (1997). The approach to the interaction between noise and other threshold-elevating variables (e.g., age) suggested by Humes and Jesteadt is conceptually consistent with the approach of Bies and Hansen (1990). While the Bies and Hansen results were challenged by Macrae (1991) using recently-acquired human data, a subsequent paper by Bies (1994) showed that, with minor modification, his alternate view of the ISO data base was also consistent with Macrae's data. It is clear that, based on the above, the ISO energy-based approach is not **unique** and other formulations, using the same database, will produce divergent estimates of NIHL. In addition, the enormous variability seen in the hearing loss data that were incorporated into the ISO-1999 standard (Mills et al., 1996) severely limits the predictive value of the approach embodied in this document. Records of litigation over the past 20 years will

confirm the diversity of strongly held opinions regarding the predictive accuracy of ISO 1999 and hence its practical utility. Clearly, a better predictive strategy, utilizing more sophisticated statistical techniques and incorporating more essential exposure variables is needed.

The number of animal model experiments has increased dramatically since the early 1970's. These studies have served to demonstrate very effectively the complexity of NIHL and have, as a consequence, altered our perspective on NIHL. Unfortunately, to date animal data have, arguably, had little effect on noise exposure standards. Based on these animal model results, it is now clear that characterizing a noise exposure by an energy metric is inadequate in many, if not most, industrial/military situations. One of the most important, although not surprising findings is the significant role of temporal variables in the production of NIHL. Since the energy approach, inherent in most criteria including ISO-1999, integrates across time, an energy metric is insensitive to the temporal structure and presentation sequence of an exposure (Lei, et al., 1994).

One key to the problem lies in the role of temporal variables and how they can be quantified. Temporal variables manifest themselves in essentially two ways: (1) in the structure of an uninterrupted noise and (2) in the sequencing of a series of discrete exposures. In the former case it is the non-Gaussian noises typical of many industrial and military environments that are most interesting. Lei et al. (1994) and Hamernik and Qiu (2001) have shown, in a series of equal energy noise exposures, that a statistical metric, the kurtosis, computed on both the time and frequency domain signal was well correlated with both the magnitude and frequency specificity of the noise-induced trauma. The kurtosis, which is defined as the ratio of the 4^{th} order central moment to the squared 2^{nd} order central moment of the sampled distribution, incorporates both the peak and interpeak interval histogram characteristics of a time varying signal. These results suggest that a statistically based metric such as the kurtosis in combination with an energy metric may be more predictive of NIHL.

Price and Kalb (1991) built a model to predict the hazard of noise exposure to high-level military-type impulse noise (the model should be applicable to more general exposure paradigms). The Price and Kalb model has a number of attractive features including nonlinear middle ear effects but it is still limited by current incomplete models of cochlear mechanics and an assumed relation between cochlear mechanics and trauma. The model is currently available only for the cat, for which there is a very limited database. The model thus could not be tested in other species for which a considerable body of data exists and under a variety of noise exposure conditions.

Over the past 25 years, a considerable body of data has accumulated on the response of the chinchilla auditory system to various noise exposures. Our laboratories alone have a database consisting of over 2500 animals exposed to continuous, Gaussian and non-Gaussian (complex), impulse or impact noises for various periods of time on an interrupted and uninterrupted exposure schedule. Additional relevant data on NIHL from several hundred additional chinchillas can be gleaned from the literature. An effort should be made to use this database, as well as that of other laboratories, to develop more sophisticated approaches to the generation of noise exposure standards.

Statistical approaches to the prediction of NIHL: An important goal in industrial health/hazard management as well as in applied NIHL research is the construction of a reliable model to predict with some precision NIHL from a set of given noise exposure parameters. Building a prediction model is a regression problem, i.e., an estimation of an unknown continuous function from a finite set of noisy samples. ISO 1999 as well as other predictive schemes or DRCs have applied the so-called 'first-principle model' (Cherkassky and Mulier, 1998). This approach is a distribution-based statistical technique that tries to mechanically fit a pre-specified function to some data set. Most NIHL research results, including all of our previous work, are based on a first-principle approach. This approach works well when the

number of samples is large relative to the model complexity. However, even when the number of samples is very large, this method can produce a large bias if the model complexity is incorrectly selected or the system under study is too complex to be mathematically described. The prediction of NIHL under various noise exposure conditions is just such a problem. There is a growing consensus that it is impossible to use a few simple parameters, such as energy and exposure duration, to predict hearing hazards with any precision from the large diversity of complex noise environments. New statistical approaches such as the artificial neural network (ANN) and support vector machine (SVM) learning algorithms, which can develop models from large, complex and information-rich data sets are available and have been successfully used to solve complex nonlinear problems in science and engineering. Among the most attractive features of such approaches is that they are distribution-free models that learn directly from the input data. While such models cannot provide information on the mechanisms of NIHL (nor should they be expected to), they may be extremely useful in predicting the outcome of an exposure from the appropriate input parameters.

The ANN: An artificial neural network is a network of processing units each of which has some properties that are similar to those of biological neurons. An ANN is a computing device that mimics our inferred understanding of information processing and knowledge acquisition in the brain. In contrast to modern digital computers that rely on binary arithmetic in conjunction with sophisticated programming that incorporates solution procedures explicitly expressed in terms of logical statements, an ANN extracts relations from complex systems where explicit procedures cannot be "spelled out." Functionally, ANNs can formulate relations or procedures of operation by "learning" from input data (examples). An ANN can be trained to recognize patterns in an incomplete data set.

In a complex system such as the mammalian auditory system, in which an output (response) is dependent on the complex interactions among various input parameters, a conventional systems analysis approach, which relies on mathematically tractable relations, may not be appropriate. Rather an ANN approach can be used to search for a relation among data sets in an adaptive and "fuzzy" manner. That is, an ANN approach is advantageous in the handling of problems where explicit rules are not easily formulated. This search operation can be achieved with an incomplete data set through the self-learning and associative abilities of an ANN. Thus the relation between noise metrics and auditory system changes can be obtained using an ANN approach without the restrictions imposed by a traditional mathematical approach requiring tractable functions, provided that sufficient training data are available.

As in nature, a network function is determined largely by the connections between elements. One can train a neural network to perform a particular function by adjusting the values of the connections (weights) between elements. It is apparent that an ANN derives its computing power through, first, its massively parallel distributed structure and, second, its ability to learn and therefore generalize. These two information-processing capabilities make it possible for ANN to solve complex problems that are currently intractable.

The SVM: The support vector machine is a universal constructive learning procedure based on Vapnik's statistical learning theory (Vapnik, 1995), which can learn a variety of representations, such as neural nets, polynomial models, radial basis functions and splines. Moreover, SVM itself can be viewed as a promising method for pattern recognition tasks or regression problems. The SVM also has advantages in higher dimensional spaces because the optimization of the machine does not depend on the dimensionality of the input space. This feature is especially suitable to our research on noise hazard prediction.

(2) Significance: There is consensus of opinion on the need to be able to predict the effects of a noise exposure, but there is as yet no generally agreed upon method for accomplishing this. In this research we developed modern statistical learning models to predict noise-induced effects on the

peripheral auditory system in an animal model. The models were trained by a very large and very diverse data set acquired from chinchilla studies (N > 900). The success of this initiative demonstrates the feasibility of such an approach. Because of the similarity of the chinchilla and human response to noise the demonstration of the feasibility of such a modeling approach can form the basis for creating a predictive model applicable to humans and can lead to a new approach to creating a DRC.

The successful development of a predictive scheme will also be cost effective in the long run by reducing the number of parametric studies that need to be carried out in order to determine the effects of new and suspect noise environments. Since this model can be used to identify noise parameters and combinations of parameters important in determining trauma, critical animal model experiments that should be performed can be identified. Thus, an additional benefit of this research will be to reduce the number of animals that need to be used in noise research.

III. Experimental Design and Methods:

Our statistical learning models were developed using three structures: (i) a feed-forward neural network, (ii) a Gaussian radial basis function neural network and (iii) a support vector machine. The reason for using these algorithms is that both ANN and SVM are powerful tools for nonlinear problems. Our aim was to develop an optimal prediction model from these approaches.

The development of a prediction model for noise-induced hearing loss consisted of two phases: (1) model structures and their algorithm designs and (2) experimental design. Each of these phases is described below.

(1) Model structures and corresponding algorithm designs:

Two inductive principles were used in adaptive model estimation: the regularization inductive principle (including the cross validation technique) for two ANN models and structural risk minimization (SRM) for the ANN and SVM models. Table 1 outlines all three adaptive regression approaches and algorithms for model selection (i.e. choosing optimal model complexity) and parameter estimation that were used in this research.

Table 1. Three adaptive regression approaches and related algorithms.

Adaptive regression approach	Algorithm/principle(s) for model selection	Algorithm for parameter estimation
(A) Feed-forward neural network	(1) Cross validation (2) SVM	Back propagation algorithm for all weights in both hidden and output layers
(B) Gaussian RBF neural network	(1) Cross validation (2) SVM	(1) *k*-means clustering algorithm/ SVM for RBF centers (2) Back propagation algorithm for weights in output layer
(C) Support vector machine (SVM)	SRM and Vapnik's loss function	Quadratic programming algorithm in the kernel representation

Three optimal prediction models using the above three adaptive regression approaches were obtained. In the last phase of this research, the performance of the three models was compared. The best one was selected as our final prediction model for noise-induced hearing loss.

(a) Feed Forward ANN With A Back Propagation (BP) Algorithm:

In the multilayer feed forward topology, the inputs that are presented to each perceptron (a computing element/neuron in the ANN) only come from connections with the preceding layer. A schematic of such a multilayer perceptron network (MLP) (Hush & Horne, 1993; Dayhoff, 1990) is shown in Fig. 1. In this figure, each circle represents a perceptron, and the arrows indicate connections between perceptrons. The input vector feeds into each of the first layer perceptrons comprising the input layer. The input layer is passive, in that it merely receives the data patterns passing into the network. The output of this layer feeds into each of the second layer perceptrons and so forth. The output layer yields the network's result. Between the input and output layers there are one or more intermediate layers referred to as hidden layers. Each layer may have a different number of neurons, and even a different transfer function. Hornik et al., (1989) proved that a two-layer network (the input layer is not included), with sigmoid transfer functions in the hidden layer and linear transfer functions in the output layer, can approximate virtually any function of interest to any degree of accuracy, provided sufficiently many hidden units are available. The sigmoid function is a nonlinear activation function defined by the logistic function:

$$f(x) = \frac{1}{1 + \exp(-x)} \tag{1}$$

The development of the back propagation (BP) algorithm represents a landmark in the design of neural networks in that it provides a computationally efficient method for the training of multilayer perceptrons (Haykin, 1999). The BP algorithm essentially compares the actual output of the MLP with the desired output (known from training data). In the structure of an MLP network any changes in the weights produces a chain reaction of effects that propagates forward through the successive layers of the network. The BP algorithm starts to adjust the weights at the last hidden layer (i.e. the layer immediately behind the output layer) and continues to make adjustments successively toward the first hidden layer (i.e. the layer immediately following the input layer). The calculations used to obtain the weight adjustments at a given layer are used in computing the adjustments for the next layer and so forth until the input layer is reached.

The BP algorithm for a MLP network is actually a generalization of the least mean square (LMS) algorithm developed by Widrow and Hoff (1960). The standard BP algorithm is a gradient descent algorithm in which the network weights are moved along the negative of the gradient of the performance function. When the LMS is used for the single-layer linear network the mean squared error is a quadratic function so that it is guaranteed to converge to a solution that minimizes the mean squared error as long as the learning rate α is not too large. However, in a multilayer nonlinear network the situation is more complicated. The performance surface for a multilayer network may have many local minimum points and the curvature can vary widely in different regions of the parameter space. There are a number of variations on the basic algorithm that are based on heuristic modifications to the basic BP and other numerical optimization techniques, such as the conjugate gradient and Newton's methods (Hagan et al., 1996; Haykin, 1999; Demuth and Beale, 2000). After comparing performances of a number of BP algorithms, the Levenberg-Marquardt algorithm (Hagan et al., 1996; Scales, 1985) was selected as the main algorithm for building our multilayer network prediction model. The reason for selecting this

algorithm is its fast convergence and accurate training ability for networks containing up to a few hundred weights.

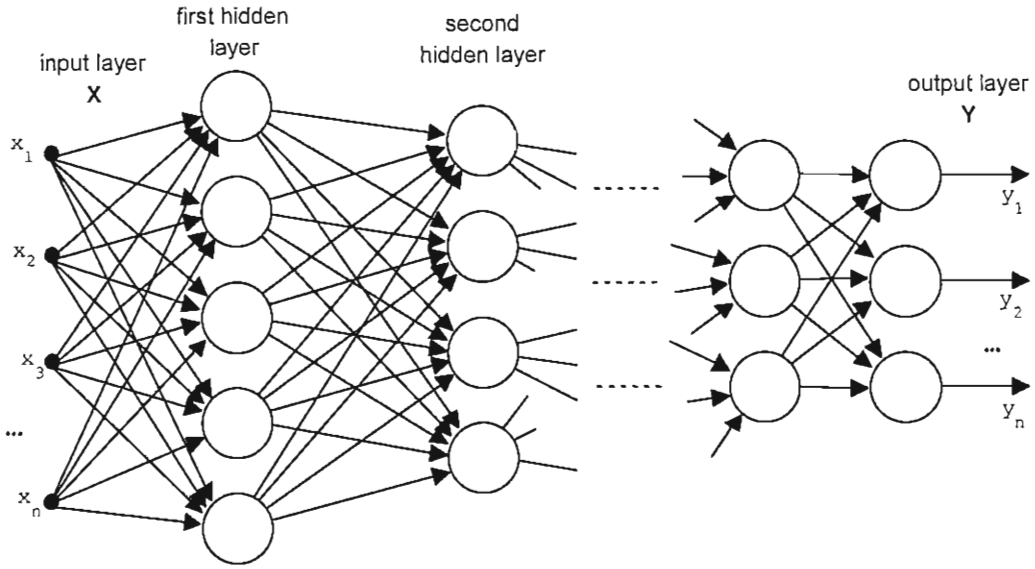

Fig. 1 Architecture of an MLP feed forward network.

- Network structure:

The universal approximation theorem (Hornik et al., 1989; Haykin, 1999) states that a single hidden layer is sufficient for a multilayer network to approximate any function of interest to any degree of accuracy, provided sufficiently many hidden units are available. However, the theorem does not state that a single hidden layer is optimum in the sense of learning time, ease of implementation, or generalization. Theoretical results and many simulations in different engineering fields have shown that there is no need to have more than two hidden layers for a multilayer network to approximate any function (Kecman, 2001). The problem in our design is whether one or two hidden layers should be used. Both architectures are theoretically able to approximate any continuous function to the desired degree of accuracy (Cybenko, 1989; Hornik et al., 1989; Kurkova, 1992). It is difficult to establish, a priori, which topology is better. Therefore, in our modeling efforts we tried both structures and found that the performance of the structure with two layers was not significantly better than the one with one layer (see "MLP neural network model selection" on page 24~25).

- Model selection:

In the case of general nonlinear regression, the mean squared error (MSE) could be decomposed into bias and variance components. If the parameters give a low bias the approximation error arises from a high variance, and vice versa. This is referred to as the bias-variance dilemma (Geman et al., 1992). A trade-off must be made between these two components. Cross validation technique was used to resolve this design problem.

Cross validation technique:

Cross validation is a statistical method to resolve the trade-off between bias and variance (Cherkassky and Mulier, 1998; Kecman, 2001). In the cross validation approach the available training data set is randomly partitioned into two subsets: a learning set and a validation set. The learning data are used to separately estimate a number of different models (a single and two

hidden layers with different number of neurons in our case) while the validation data are used for testing the model. The estimated model with the best average performance would be selected as the final prediction model.

The k-fold cross validation approach was used for model selection. For a given data set $z=[x,y]$, where $x=[x_1, \ldots, x_n]$ and $y=[y_1, \ldots, y_n]$ of sample size n, the squared error loss functions of m candidate network structures are computed as following (Cherkassky and Mulier, 1998):

1. Randomly divide the training data z into k disjoint samples of equal size $\mathbf{z}_1, \mathbf{z}_2, \ldots, \mathbf{z}_k$.
2. For each validation sample z_i of size n/k

   a. Use the remaining data, $z_l = \bigcup_{j \neq l} z_j$ to construct an estimate f_i.

   b. For the regression estimate f_i, sum the empirical risk for the data z_i, which is not used to estimate the model:

$$r_i = \frac{k}{n} \sum_{z_i} (f_i(x) - y)^2 \tag{2}$$

3. Compute the estimate for the prediction risk by averaging the empirical risk sums for z_1, $z_2, \ldots, z_k$:

$$R_{ml} = \frac{1}{k} \sum_{i=1}^{k} r_i \tag{3}$$

where m indicates the number of candidate models. The model with minimum R was selected as the multilayer prediction network. If the performance of the top three models was very close, the model with simplest structure was selected as the prediction model.

Two-thirds of the data set was randomly partitioned as the training and validation data sets and the remaining one-third as the test data set. Considering that all the data sets came from different types of noise, the database was stratified according to the exposure noises before sampling to make sure that the samples from different types of noise are allocated to both training and test data sets more or less equally. For the training data (2/3 of the database) two data division techniques were used to build the best prediction model using a MLP feed-forward network:

Universal model

Neglecting the fact that all available training data are collected under different exposure conditions, the training data is randomly divided into k (k= 5 or10) disjoint samples of equal size $z_1, z_2, \ldots, z_k$. Use the above approach to get a universal model.

Specific model

The fact that all available data come from different exposure conditions was considered in this approach. The database was stratified before sampling. In this case we set k (k=4~6). For each subset under a certain exposure condition, the training data was randomly divided into k disjoint samples. Then randomly divided samples were picked from each subset by sampling without replacement to form k disjoint samples of z_1, $z_2, \ldots, z_k$ (note the size of each z_i is not necessarily equal but will be quite close). The same approach as above was used to get the specific prediction model.

- Weight initialization

  Choosing the initial weight (and bias) is an important step in getting good network performance. A sigmoidal function was selected as the activation function in our multilayer prediction model. The basic strategy in choosing the initial weight should ensure that after initialization most of the sigmoidals are not too steep and that they are inside the domain of the approximated data points. In our case the initialization of weight was processed as follows:

  For the initialization weight in the hidden layer(s), the initial weights were generated by a normal distribution with a zero mean and with a standard deviation σ that is proportional to $1/I^{-1/2}$ (I is the dimension of the input) for the normalized input vectors, to ensure that the activation of the hidden neurons is determined by the nonlinear parts of the sigmoidal functions without saturation (Bishop, 1995).

  For the initialization weight in the output layer, and to avoid small weights, half the weights should be initialized with +1, and the other half with –1. If there are an odd number of output layer weights, then the bias should be initialized at zero (Smith, 1993).

- Data preprocessing

  To make the neural network training more efficient some preprocessing on the samples was performed.

  1) Data normalization: Since the sigmoidal function is in the range [-1,1], the training pair [x,y] was normalized to the range [-1,1];

  2) Principal component analysis: This technique was used to orthogonalize the components of the input vectors so that they are uncorrelated with each other.

(b) Radial Basis Function Neural Network (RBFNN)

Like a multilayer perceptron (MLP), an RBF network has a universal approximation ability (Hartman et al., 1990; Park and Sandberg, 1991). The RBFNN (Fig. 2) is a multilayer feed forward neural network consisting of an input layer of source nodes, a layer of non-linear hidden units that operate as kernel nodes and an output layer of linear weights. Cirosi and Poggio (1990) showed that an RBF network has the best approximation property of all neural network structures. Thus the RBF network was selected as a candidate tool for our prediction model.

A generalized regression neural network (RBFNN) is frequently used in function approximation, the architecture of a RBFNN is shown in Figure 2. A RBFNN has two layers, one is radial basis layer and the other is a special linear layer.

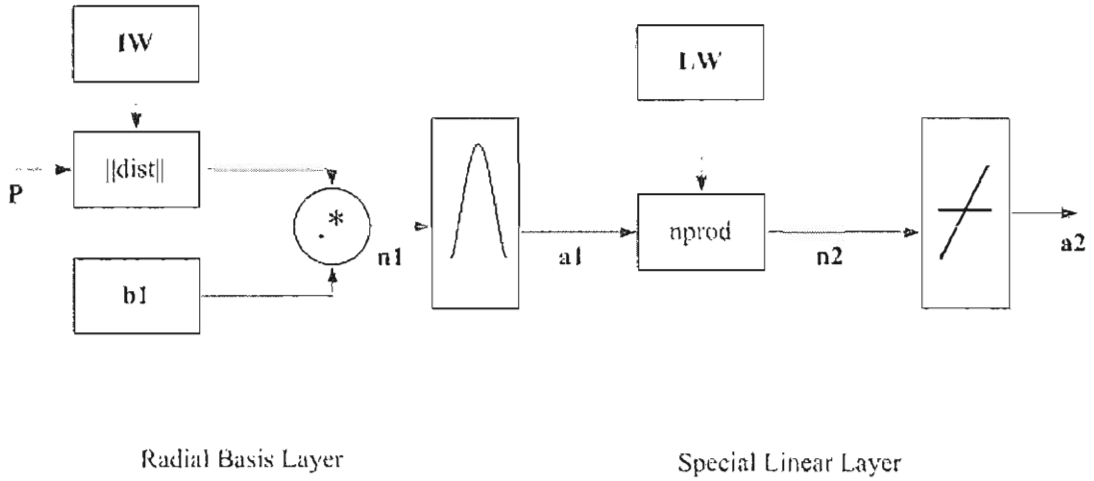

Fig. 2 Architecture of a RBFNN.

The ||dist|| box in the figure accepts the input vector **p** and the input weight matrix **IW**, and produces a vector having S elements. The elements are the distances (dot products) between the input vector and the vectors **IW** formed from the rows of the input weight matrix. The bias vector **b**1 and the output of ||dist|| are combined by the element-by-element multiplication. The values of 'distances' are fed into radial basis neurons. The transfer function of the radial basis neuron is:

$$radbas(x) = e^{-n^2} \tag{4}$$

The radial basis neurons with weight vectors quite different from the input vector will have outputs near zero, and the small outputs will only have a negligible effect on the linear output neurons. On the other hand, a radial basis neuron with a weight vector close to the input vector will yield a value near 1. If a neuron has an output of 1 its output weights in the second layer pass their values to the linear neurons in the second layer.

In the first layer, each neuron's weighted input is the distance between the input vector and its weight vector, and its net input is the element by element product of its weighted input with its bias. If a neuron's weight vector is equal to the input vector, its weighted input will be zero, and its output will be 1. If a neuron's weight vector is a distance of spread from the input vector, its weight input will be spread, its net input will be root square of -log(0.5) (or 0.8326), such that its output will be 0.5. The value of spread can be adjusted according to the performance of the networks. The RBF network takes matrices of training input vectors **P** and target vectors **T,** and a spread constant for the radial basis layer, and return a network with weights and biases such that the output are exactly **T** when the input are **P.** The number of neurons is the same as the number of training input vectors **P** and the first layer weights are set to **P'**. Each bias in the first layer is set to 0.8326/SPREAD, this determines the width of an area in the input space to which each neuron responds. The value of SPREAD should be large enough that neurons respond strongly to overlapping regions of the input space. This will make the network function smoother and results in better generalization for new input vectors occurring between input vectors used for constructing the network.

One concern for this kind of RBF network may be the number of hidden neurons, since it has as many as input vectors. On the other hand, it takes much less time to construct a RBF network than training a sigmoid/linear network.

The second layer has as many neurons as input/target vectors, and **LW** is set to **T**. The nprod box produces S2 elements in vector n2. Each element is the dot product of a row **LW** and the input vector **a1**, all normalized the sum of the elements of **a1**. If an input vector p close to a training input vector p0, this vector p will produce a layer 1 output close to 1, and this leads to a layer 2 output close to t0, one of the targets used in training the network.

(c) Support Vector Machine (SVM):

As discussed above an appropriate ANN should balance the bias and variance, trying to keep each as low as possible. When the data set is large enough (goes to infinity) a neural network can approximate any regression function to an arbitrary degree of accuracy. Unfortunately, in practice the size of the data set usually limited. By taking into account the size of the data set, which is often small with respect to the problem's dimensionality, it is advantageous to consider some approaches to learning that are based on small sample statistics. A support vector machine (SVM) approach is just such a statistical learning technique.

The support vector machine is a new learning machine based on statistical learning theory developed by Vapnik and Chervonenkis (Vapnik, 1995). The term *support vector* indicates a subset of the training data corresponding to the solution of the learning problem. The fundamentals of SVM are structural risk minimization (SRM) and Vapnik-Chervonenkis (VC) bounds.

Least-square support machine vector (LS-SVM) was used in our research. LS-SVM (Suykens 2002) is a modification to the Vapnik SVM . The modifications are in two folds. First, equality constraints are taken instead of inequality constraints. With this modification, the threshold in the SVM inequality constraints can be considered as a target value, with which an error variable e_k is allowed to tolerate the estimation errors. Second, a squared loss function is taken for the error variable. The modifications will greatly simplify the original SVM problem.

Consider the function in the primal weight space:

$$f(\mathbf{x}) = \mathbf{w}^T \varphi(\mathbf{x}) + b \tag{5}$$

where $\mathbf{x} \in R^n$, $y \in R^1$ and $\varphi(.) : R^n \rightarrow R^1$ is the mapping to the high dimensional and potentially infinite dimensional feature space. The optimization problem in the primal weight space can be formulated as follows giving the training set $\{\mathbf{x}_k, y_k\}, k = 1,...N$:

$$\min_{w,b,e} J_P(\mathbf{w}, e) = \frac{1}{2}\mathbf{w}^T\mathbf{w} + \gamma\frac{1}{2}\sum_{k=1}^{N} e_k^2 \tag{6}$$

such that $y_k = f(\mathbf{x}_k) = \mathbf{w}^T \varphi(\mathbf{x}_k) + b + e_k, k = 1,..., N$

The Lagrangian is constructed as:

$$L(\mathbf{w},b,e;\alpha) = J_p(\mathbf{w},e) - \sum_{k=1}^{N} \alpha_k (\mathbf{w}^T \varphi(\mathbf{x}_k) + b + e_k - y_k) \tag{7}$$

where α_k are Lagrange multipliers. The conditions for optimality are given by

$$\frac{\partial L}{\partial \mathbf{w}} = 0 \rightarrow \mathbf{w} = \sum_{k=1}^{N} \alpha_k \varphi(\mathbf{x}_k) \tag{8}$$

$$\frac{\partial L}{\partial b} = 0 \rightarrow \sum_{k=1}^{N} \alpha_k = 0 \tag{9}$$

$$\frac{\partial L}{\partial e_k} = 0 \rightarrow \alpha_k = \gamma e_k, k = 1,...,N \tag{10}$$

$$\frac{\partial L}{\partial \alpha_k} = 0 \rightarrow \mathbf{w}^T \varphi(\mathbf{x}_k) + b + e_k - y_k = 0, k = 1,...,N. \tag{11}$$

$$K(\mathbf{x}_k, \mathbf{x}_l) = \Omega_{kl} = \varphi(\mathbf{x}_k)^T \varphi(\mathbf{x}_l), k,l = 1,...,N \tag{12}$$

We get the following solution:

Solve in α, b:

$$\begin{bmatrix} 0 & 1_v^T \\ 1_v & \Omega + I/\gamma \end{bmatrix} \begin{bmatrix} b \\ \alpha \end{bmatrix} = \begin{bmatrix} 0 \\ y \end{bmatrix} \tag{13}$$

where $y = [y_1;...;y_N]$, $1_v = [1;...1]$ and $\alpha = [\alpha_1;...\alpha_N]$. The kernel is obtained as follows:

$$K(\mathbf{x}_k, \mathbf{x}_l) = \Omega_{kl} = \varphi(\mathbf{x}_k)^T \varphi(\mathbf{x}_l), k,l = 1,...,N \tag{14}$$

The resulting LS-SVM model for function estimation becomes

$$f(\mathbf{x}) = \sum_{k=1}^{N} \alpha_k K(\mathbf{x}, \mathbf{x}_k) + b \tag{15}$$

where α_k, b are the solution of the linear system. The parameters can be determined by exploring a training set, validation set and testing set. The values of the parameters are selected such that the best performance on this validation set has been achieved. To avoid the performance being too sensitive with respect one particular validation set, *n*-fold cross-validation approach could be adopted.

If an RBF kernel $K(\mathbf{x}, \mathbf{x}_k) = \exp\left(-\frac{|\mathbf{x} - \mathbf{x}_k|^2}{\sigma^2}\right)$ is selected, then only two parameters (γ, σ) need to be tuned.

(2) Experimental Design:

The experimental design includes: (a) selection of dependent and independent variables (b) database organization; (c) frequency considerations in the prediction model; (d) model validation and the performance metric.

(a) Selection of dependent and independent variables:

The proposal takes advantage of a large existing experimental database to create a 'universal' prediction model (for the chinchilla) that can evaluate hearing hazard not only caused by steady state noise but also non-stationary noise, such as impulse/impact and other categories of non-Gaussian noises. The database was analyzed using modern adaptive regression techniques. The approach used two types of artificial neural networks and a support vector machine. Each of these promising algorithms has its advantages (as discussed above). The final model chosen was the one showing the best performance in terms of predictive accuracy. Table 3 lists all of the dependent and independent variables for the prediction model. Some discussion of these variables follows.

Selection of variables: The variables listed in Table 2 are, except for the kurtosis variables, the generally accepted variables for defining noise exposures for purposes of hearing conservation practice as well as those for specifying noise-induced effects. An extensive literature supports this assertion. Our recent papers support the inclusion of the statistical metric -- kurtosis.

Table 2 Inputs and outputs for the prediction models.

Inputs (independent variables)	Outputs (dependent variables)
Noise metrics: 1. Weighted energy, $E_w(t)$; 2. Kurtosis in time domain, $\beta(t)$; 3. Probability of a transient occurring in impulse/impact noise, P; 4. Kurtosis in frequency domain $\beta(f)$ at cf = 0.5, 1, 2, 4, 8 kHz; 5. Weighted energy in filtered octave bands $E_w(f)$ at cf = 0.5, 1, 2, 4, 8 kHz; 6. Noise type, N_T; 7. Impulse peak pressure, P_{peak}; 8. Impulse duration, D; 9. Impulse number, N; 10. The energy of background noise, $E_b(t)$; Biological input variables: 1. Pre-exposure auditory evoked potential thresholds, $PRE_{EP}(f)$ at cf = 0.5, 1, 2, 4, 8 kHz; 2. Temporary threshold shift, $TS(f)$ at cf = 0.5, 1, 2, 4, 8 kHz 3. Pre-exposure cubic distortion product otoacoustic emission, $PRE_{DPOAE}(f)$ at cf = 0.5, 1, 2, 4, 8 kHz.	Indices of trauma to the auditory system (at specific center frequencies): 1. Noise-induced PTS, $PTS(f)$ (dB) at cf = 0.5, 1, 2, 4, 8 kHz; 2. Outer hair cell loss, $OHC(f)$(%) at cf = 0.5, 1, 2, 4, 8 kHz; 3. Inner hair cell loss, $IHC(f)$ (%)at cf = 0.5, 1, 2, 4, 8 kHz; 4. Permanent change in DPOAE, $\Delta DPOAE(f)$ (dB) at cf = 0.5, 1, 2, 4, 8 kHz.

Independent variables (inputs to the model):

Noise metrics (exposure parameters):

(1) Weighted energy, $E_w(t)$: It is well accepted that energy is an important predictor for assessing hearing hazard. Energy is the basis of the 1968 and 1990 criterion. Since hazard depends on both sound pressure and some function of time, a time integrated exposure level was used (ISO, 1990):

$$E_X = 10\log_{10}\frac{1}{T}\int_0^T \frac{[P_X(t)]^2}{P_0^2}dt + 10\log_{10}(\frac{T_N}{T_0}) \tag{16}$$

where T is the duration of the exposure, T_N is the specified duration of the exposure in suitable units of time, and P_0 is the reference rms sound pressure (re 2×10^{-5} pascals). In the equation, P_x is the instantaneous (weighted or unweighted) sound pressure in pascals. The use of "X" as a subscript in the above refers to the weighting function that will be used: A-weighting and/or P-weighting function. A weighting function essentially assigns factors to the various spectral components of a stimulus that are proportional to the ability of that frequency to produce hearing loss.

A-weighting is the most commonly used function, and has been incorporated into most sound level meters. A-weighting of steady G noise provides a good estimate of the relative hazard to hearing of the various frequencies that compose a steady noise exposure (Mills et al., 1983). However, A-weighted sound exposure level (SEL) will tend to overestimate the hazard from impulses with large amounts of low-frequency energy (Patterson et al., 1993). Patterson et al., 1993 established an empirical P-weighting function based on 475 chinchillas that were exposed to a variety of impulse noises. P-weighting provided a more accurate assessment of the hazard from such impulses. However, since the number of animals and exposure conditions used to derive the P-weighting function were limited, its generality could not be confirmed. Our previous work (Patterson and Hamernik, 1992; Patterson et al., 1993) showed that the appropriate weighting function for impulse containing noises is not a simple monotonic function, as implied by A-weighting, but rather a more complex function at frequencies above approximately 1 kHz.

(2) Kurtosis in time domain, $\beta(t)$: The kurtosis is defined as the ratio of the fourth-order central moment to the squared second-order central moment of the distribution, i.e.:

$$\beta(t) = \frac{\sum_{k=0}^{N-1}(x_k-\mu)^4}{\sum_{k=0}^{N-1}(x_k-\mu)^2} \tag{17}$$

where μ is mean of x_k, k= 0,1,…, N. For a Gaussian distribution the kurtosis is 3. Erdreich (1986) suggested using kurtosis to characterize impulse exposures. Most of the industrially relevant noises can be modeled as combinations of Gaussian noise with a variety of transients mixed in. It is the transients either impacts or noise bursts that give the noise its non-G character. The kurtosis of a sampled signal provides information about the duration of any transients in the noise, the repetition rate of the transients, the relative difference between peak and background levels and the peak intervals in the analysis window. In our previous work (Hamernik et al., 2003) we found that a 40-s analysis window for kurtosis calculation is adequate. This and other related work referenced in the above paper indicated a high correlation between trauma and β(t).

(3) Probability of a transient occurring in a non-Gaussian exposure, P and the peak/interval histogram: Recent research (Hamernik et al., 2003) has shown that the probability of a transient occurring is an

important variable in determining trauma. This might be expected since in the limit as P goes to zero, a non-G exposure approaches the G condition. These results also show that an asymptotic limit of cell or hearing loss for $\beta(t)$>~40 at a given Leq holds across a series of exposure conditions that had very different peak as well as interval histograms but the same energy. This is significant because it suggests that the temporal and peak sequencing of transients does not have an appreciable effect on indices of trauma (at least as far as industrial noise is concerned) over a realistic, although not all inclusive, range of these variables. Over the years a number of studies have looked separately at the effects of impact peak SPL or at the effects of varying the inter-stimulus interval (ISI) both of which were typically held constant in any given exposure condition. Such exposures, as far as industrial noise issues are concerned, are rather unrealistic. So too was the omission of any background noise in the exposure paradigm. The asymptotic behavior of the non-G exposure data in Hamernik et al., (2003) through to the pure impact exposure end point of the exposure sequence suggests that these variables may not need to be considered when evaluating industrial noise for hearing conservation purposes. Their contribution, as well as that of other time related factors, is buried in the statistical metric $\beta(t)$.

The probability of a transient occurring could be calculated from the joint peak-interval histogram (Lei and Hamernik, 1998) by averaging several analysis windows.

(4) Kurtosis in frequency domain, $\beta(f)$: It has been generally accepted that the spectrum of the noise is an important feature for trauma assessment (Kryter, 1970; Price 1983, 1986; Hamernik and Qiu, 2001). Time domain kurtosis $\beta(t)$ is not sensitive to frequency components of a non-G noise. Hamernik et al., (1998, 2001, 2003) found the kurtosis computed on the filtered octave band noise signal, $\beta(f)$, was useful in the prediction of the place-specific outer hair cell loss and PTS.

(5) Weighted energy in filtered octave bands, $E_w(f)$: $E_w(f)$ is an important determent of trauma. In our research plan both $\beta(f)$ and $E_w(f)$ was used together to predict PTS, OHC/IHC loss or ΔDPOAE at specific frequencies.

(6) Noise type, N_T: Since the purpose of this proposal is to establish a general animal (chinchilla) prediction model of hearing hazard for any noise environment it is important to identify the noise type (e.g., continuous, impact, impulse, interrupted, intermittent,) before inputting independent variables into the model. For example, it has been shown (e.g. Ward, 1991; Hamernik et al., 1994, 1998) that the hearing hazard produced by an interrupted exposure paradigm is generally less than that produced by an equal-energy uninterrupted exposure. This trauma reduction may also be related to the toughening phenomenon. [Note: Noises of sufficient intensity, presented to a subject on a daily repeated cycle, produce a threshold shift (TS) following the first day of the exposure. TSs measured on subsequent days of the exposure sequence have been shown to decrease relative to the initial TS. This reduction of TS, despite the continuing daily exposure has been called a cochlear toughening effect and the interrupted exposures referred to as toughening exposures.] Whether or not toughening produces a protective effect, i.e., less PTS from the exposure producing the toughening or from a subsequent exposure, is not entirely clear. In the research plan some physiological phenomena, such as acoustic reflex and toughening, are expected to be absorbed into modern statistical algorithms by supplying the noise type information to the model.

Some noise types N_T in the database include: (1) a single short (acute) exposure (a few milli seconds to 8 hr.) (2) different on-fractions, (3) intermittent noise (quiet intervals of a few seconds to an hour), (4) interrupted noise (quiet intervals of several hours), (5) continuous noise (uninterrupted for up to 5 days).

(7-10) Impulse peak pressure, P_{peak}; Impulse duration, D; impulse number, N, and the energy of background noise, $E_b(t)$: Although $\beta(t)$ incorporates the variables of P_{peak}, D and N, it cannot provide any

specific information on these variables. It is well known that taken individually each of these variables has an effect on the degree of trauma. Erdreich (1986) suggested using kurtosis to define an impulsive noise environment, but he indicated that the contribution of level, spectrum and peak distribution to the biological effect needed to also be individually evaluated. From our experience with non-G simulation, different combinations of peak distribution, impulse duration, background noise, and probability of a transient occurrence could produce the same kurtosis in time domain but different effects on hearing. Therefore, variables of impulse peak pressure P_{peak}, impulse duration D, impulse number N and the energy of background noise $E_b(t)$ were used to complement the kurtosis metric.

Biological input variables:

(1) Pre-exposure auditory evoked potential thresholds, PRE_{EP}: Even under the same exposure conditions, the variability between subjects is often very large. There are a number of possible causes one of which has been the preexposure thresholds. Since these data are readily available they were used as inputs to the model.

(2) Temporary threshold shift, *TTS*: Since it seemed reasonable to assume that temporary losses of hearing were somehow related to permanent losses (Reger and Lierle, 1954), TTS experiments became very popular in humans and other animals for a number of years. While a considerable amount has been learned about the behavior of TTS and its relation to exposure parameters, the results have arguably had a modest impact on our knowledge of how NIPTS accumulates over a working lifetime. Our recent work on 900 chinchillas (Hamernik et al., 2002) showed that across audiometric test frequency, there was a consistent relation between threshold shift (TS) and PTS of the form

$$PTS(\text{dB}) = a(e^{TS/b} - 1) \tag{18}$$

where, for a given test frequency, a (dB) and b (dB) are constants. Correlation between TS and PTS at the various test frequencies was the highest for TS_{24}, where TS_{24} was measured 24 h after exposure. The variable TS_{24} was used as an additional parameter in the prediction model.

(3) Pre-exposure cubic distortion product otoacoustic emission, PRE_{DPOAE}. Since the source of the emissions lies in the bidirectional transduction properties of the OHC (Brownell et al., 1985), emissions seemed ideally suited for the early detection of noise-induced hearing loss which typically first manifests itself in OHC changes and, in particular, the OHC cilia (Liberman and Dodds, 1984). Our previous study showed that the distortion product emissions were more sensitive, frequency-specific indices of noise-induced cochlear effects than pure-tone threshold measures. This was particularly evident near the threshold for noise-induced damage to the outer hair cell system (Hamernik et al., 1996). As with preexposure thresholds, PRE_{DPOAE}, which when taken into account, may be a useful in reducing variability.

Dependent variables (outputs of the model):

(1) NIPTS at a specified frequency, *PTS(f)*: NIPTS is the most often used index of the effects of noise on hearing in humans. All existing exposure criteria use PTS. In humans as well as other animals PTS is the only available index that is routinely used to evaluate hearing loss.

(2-3) OHC and IHC loss at a specified location, *OHC(f)*, *IHC(f)*: In animals OHC and IHC loss are often used as an adjunct to audiometric measures which often do not correlate well with the pathology. Often OHC loss is found when threshold measures are normal. The quantitative relation between sensory cell loss and hearing thresholds was shown to follow a sigmoid function (Hamernik et al., 1989):

$$\text{OHC \% loss} = 100\left[1 + e^{\left(\frac{C-\text{PTS}}{B}\right)}\right]^{-1} \tag{19}$$

where, B (dB) and C (dB) are empirically determined, frequency dependent constants. Although correlations were high, variability was large. IHC loss/PTS followed a similar relation but with poorer correlations. It is clear that the relation between PTS and OHC/IHC loss (%) is nonlinear. Kraak (1981) indicated, "as a result of exposure of the hearing organ to noise, hair cell damage may occur without the influence on hearing being measurable. In further exposure, the damage will accumulate and finally result in impairment of hearing". Sensory cell loss provides an alternative index of noise-induced effects.

(4) Permanent change of DPOAE at a specified frequency, $\Delta DPOAE(f)$: Since the effects of noise are usually first detected in the OHCs and the OHCs are generally considered to be the source of the DPOAEs, permanent change of DPOAE was used as another index of NIPTS. ΔDPOAE is defined as the difference between the frequency specific pre-exposure DPOAE and the 30d post-exposure DPOAE at the primary frequency level of $L_1=L_2=70$ dB. Data are available for other primary levels. A justification based on current literature can be made for the choice of 70 dB.

(b) Database organization:

For the past 25 years all the variables shown in Table 3 have been systematically archived. The database contains audiometric, otoacoustic emission and histological data for each animal exposed to a specific noise. All the data for each animal in the database is complete. Two individuals, prior to archiving, checked each data point. Most of these data have appeared in our published papers and reports. With Microsoft's Access all the required information can be extracted, i.e., biological input data (B_A, B_S, PRE_{EP}, TS and PRE_{DPOAE}) and indices of trauma to the auditory system at specified frequencies (PTS, OHC and $\Delta DPOAE$).

All exposure noises were recorded and digitized by computer. One of the first tasks was to analyze all the exposure noises using the digitized recorded data sets. A program was written to analyze noises using the Matlab platform. All the noise metrics listed in Table 3 were computed and input into the database.

Since some noise metrics, for example P_{peak}, D, N, P, and $E_b(t)$ are specific for non-G exposures, the model must first categorize the exposure as either G or non-G. Kurtosis in time domain, $\beta(t)$, was used to determine the nature of the exposure. The kurtosis of Gaussian steady noise is equal to 3. The non-G charater of the noise increases as $\beta(t)$ increases. If $\beta(t) \leq 3.5$ the noise was classified as steady G noise and all variables related to non-G noise was set to zero. Thus for Gaussian noise only weighted energy $E_w(t)$ and weighted energy in filtered octave bands $E_w(f)$ were used as noise metrics. This is equivalent to the traditional prediction models such as ISO 1999. Note industrial noise is not typically Gaussian.

(c) Frequency considerations in the prediction model:

Since thresholds and otoacoustic emissions are measured at multiple frequencies and OHC/IHC loss is evaluated at multiple locations that are eventually transformed to corresponding frequencies (Eldredge et al., 1981), NIHL must be evaluated in a frequency specific manner. This makes it necessary to account for possible correlation between contiguous frequency bands. Two frequency specific prediction models were considered:

(i) Specific frequency model (SF model): Five frequencies were considered (cf = 0.5, 1, 2, 4, 8 kHz). That is, a prediction model was built for each specified frequency. Hence, there were five prediction models each one good only for the specified frequency.

(ii) Wide band frequency model (WF model): In the SF model the correlation between different frequency bands, especially between contiguous frequency bands is not considered. In the WF prediction model l contiguous frequency band information on both sides of a specified frequency band was added to the input layer. For example, if 1 kHz is selected for an estimate of its indices of trauma and l=1, in the input layer, then the frequency kurtosis, energy spectra, initial AEP thresholds, etc. at cf = 0.5 and 2 kHz were also input. We will initially set l=1 since in many cases of NIHL, the most severe loss is often confined to three octaves. The average of l contiguous points (including the selected cf) will be used as the specified frequency-related inputs and outputs. At extreme points (i.e. 0.5kHz and 8 kHz) only the right or left frequency band will be added to the input layer.

(d) Model validation and the performance metric:

The rational for the 2/3-1/3 data splitting for training and verification respectively is that for statistical purposes the more data points used to train the model the better performance will be. To evaluate the model performance fairly, data for verification cannot be used in training. On the other hand, to get a good assessment on the performance of the model, more data points are needed as well. A trade off must be made to split the database reasonably. The 2/3 and 1/3 splitting, while arbitrary, is reasonable.

The metric used to evaluate the performance of the prediction models is clearly some measure of the accuracy of prediction. The error rate for each output at a specified center frequency was calculated. An average error rate over all 5-frequency bands was then obtained for each dependent variable.

Means and standard deviations for values of PTS, OHC, IHC loss and ΔDPOAE (dependent variables) for each exposure group are calculated separately and form the target values for the prediction model. The outputs of the trained prediction model for each animal in the verification set was compared to the corresponding group mean and s.d. of the dependent variables from the group to which the verifying animal belongs. If the output value is located in the range, mean ± 1s.d., the predicted value was considered correct.

To formularize the error rate the following symbols are introduced:

Y_{ij}: the values of outputs, i = 1,2,3,4 and j = 1,2,.., 5.

The output of the prediction model was four frequency-specific metrics that define hearing loss i.e. noise-induced permanent threshold shift [$PTS(f)$] at each of five audiometric test frequencies (0.5, 1.0, 2.0,4.0, and 8.0 kHz), outer hair cell loss $OHC(f)$ and inner hair cell loss $IHC(f)$ in the octave band lengths of the cochlea centered on the audiometric test frequencies, and the permanent change in the cubic distortion product otoacoustic emissions $\Delta DPOAE(f)$ at cf = 0.5, 1, 2, 4, 8 kHz. The subscript of i indicates the type of output, i.e. Y_{1j} = PTS_j; Y_{2j} = OHC_j; Y_{3j} = IHC_j and Y_{4j} = $\Delta DPOAE_j$. The subscript j indicates the specific center frequency (cf) of the octave band being considered, i.e. j = 1 to 5 corresponds to cf = 0.5, 1, 2, 4, or 8 kHz.

N_v: The total number of the animals in the verification group.

$r_l(Y_{ij})$: indicates the error rate value, of ith output at jth center frequency for Y_{ij}. The subscript l is an indicator of the animal number being used for verification, l=1,2,..., N_v.

r_i: the error rate for the four outputs i = 1, 2, 3, 4, i.e., r_1= error rate for PTS, r_2 = error rate for OHC, r_3 = error rate for IHC and r_4 = error rate for ΔDPOAE.

β_i: weighting coefficients for each of the four outputs. i=1, 2, 3, 4. The weighting coefficients are arbitrarily selected based on an inferred relative importance of the four output variables. A number of factors must be or can be considered in setting the weights. For example consider the following: (1) PTS is the generally accepted index of the effects of noise on hearing and might be considered the most important of the output variables. All existing criteria relate exposure conditions to PTS in humans. With this consideration in mind PTS might be given a strong weighting. (2) However, since PTS is often not a good index of pathology other indices of trauma have been sought. Thus, the inclusion of the DPOAE as another dependent variable but one that might be deemphasized in computing an error when the emphasis is on PTS. (3) Damage to the OHC system is the first indicator of noise trauma. This damage is not always reflected in PTS. The OHCs are the source of DPOAEs thus the latter may be more diagnostic of noise-induced change and might be given a higher weight. IHC loss is typically the least predictable of the output variables and in most situations might be heavily deemphasized. The predictive accuracy of the model can be shifted by the weighting factors dependent on the specific issue or set of issues under consideration.

Since the PTS is the most popular index used for hearing hazard, it was initially given the largest weighting followed by, OHC loss, ΔDPOAE and IHC loss.

R: the grand prediction error rate.

The error value for a given output at a specified frequency was defined in a binary manner; i.e., if the predicted value is located in the range of mean± 1s.d., the prediction error is 0. Otherwise the prediction error will be 1:

$$r(Y_{ij}) = \begin{cases} 0, (\text{mean}_{sg} - 1\text{s.d.}) \le Y_{ij} \le (\text{mean}_{sg} + 1\text{s.d.}) \\ 1, \quad \text{otherwise} \end{cases} \quad i = 1,2,3,4 \text{ and } j = 1,2,3,4,5 \tag{20}$$

where mean_{sg} is the specific group mean to which the analyzed animal belongs. The error rate for each output r_i can be expressed as:

$$r_i = \frac{1}{5}\sum_{j=1}^{5}\left\lfloor \sum_{l=1}^{N_v} r_l(Y_{ij}) \Big/ N_v \right\rfloor \quad i = 1,2,3,4 \tag{21}$$

The grand prediction error rate for the model will be:

$$R = \frac{1}{4}\sum_{i=1}^{4} r_i \tag{22}$$

The smaller the R ($0 \le R \le 1$), the better the performance of the model.

IV. Model Structure

(1) Sample number and exposure conditions:

A total 900 chinchillas, exposed under more than 130 noise environments were used to build the statistical prediction models. Among them, 578 were exposed to high level impulse noise transients, 322 were exposed to a variety of complex noises.

There are two different types of noise:

1. High level (peak>140dB) impulse noise transients with short duration, which typically occur in military environments;
2. low and medium level (peak<140dB) complex long term noise exposures (Gaussian or non-Gaussian), typical of industrial environments.

Two prediction models were designed for these two types of noise exposures. Table 3 lists the inputs and outputs variables for high level impulse noise. Table 4 indicates the inputs and outputs variables for complex noise.

Table 3. Input and output variables for high level impulse

Inputs (independent variables)	Outputs (dependent variables)
Noise metrics: 1. Weighted energy, $E_w(t)$; 2. Weighted energy in filtered octave bands $E_w(f)$ at cf = 0.5, 1, 2, 4, 8 kHz; 3. Impulse peak pressure, P_{peak}; 4. Impulse duration, D; 5. Impulse rate, R; 6. Impulse number, N; 7. Pre-exposure auditory evoked potential thresholds, $PRE_{EP}(f)$ at cf = 0.5, 1, 2, 4, 8 kHz;	Indices of trauma to the auditory system (at specific center frequencies): 1. Noise-induced PTS, $PTS(f)$ (dB) at cf = 0.5, 1, 2, 4, 8 kHz; 2. Outer hair cell loss, $OHC(f)$(%) at cf = 0.5, 1, 2, 4, 8 kHz; 3. Inner hair cell loss, $IHC(f)$ (%)at cf = 0.5, 1, 2, 4, 8 kHz;

Table 4: Input and output variables for complex noise

Inputs (independent variables)	Outputs (dependent variables)
Noise metrics: 1. Weighted energy, $E_w(t)$; 2. Kurtosis in time domain, $\beta(t)$; 3. Probability of a transient occurring, P; 4. Kurtosis in frequency domain $\beta(f)$ at cf = 0.5, 1, 2, 4, 8 kHz; 5. Weighted energy in filtered octave bands $E_w(f)$ at cf = 0.5, 1, 2, 4, 8 kHz; 6. The energy of background noise, $E_b(t)$; 7. Pre-exposure auditory evoked potential thresholds, $PRE_{EP}(f)$ at cf = 0.5, 1, 2, 4, 8 kHz; 8. Threshold shift, $TS(f)$ at cf = 0.5, 1, 2, 4, 8 kHz 9. Pre-exposure cubic distortion product otoacoustic emission, $PRE_{DPOAE}(f)$ at cf = 0.5, 1, 2, 4, 8 kHz.	Indices of trauma to the auditory system (at specific center frequencies): 1. Noise-induced PTS, $PTS(f)$ (dB) at cf = 0.5, 1, 2, 4, 8 kHz; 2. Outer hair cell loss, $OHC(f)$(%) at cf = 0.5, 1, 2, 4, 8 kHz; 3. Inner hair cell loss, $IHC(f)$ (%)at cf = 0.5, 1, 2, 4, 8 kHz; 4. Permanent change in DPOAE, $\Delta DPOAE(f)$ (dB) at cf = 0.5, 1, 2, 4, 8 kHz.

(2) Data partition methods

The samples from different groups were divided into training, validation and testing sets through two partition methods.

Method 1: Specific model

Considering that all the data sets from different types of noise, the database is stratified according to exposure noises before sampling to make sure that the samples from different types of noise are allocated to both training and test data sets more or less equally.

Method 2: Universal model

The fact that all available training data are collected under different exposure conditions is neglected. The samples from different groups are divided into 4 disjoint sample sets of equal size, z_1, z_2, z_3, z_4, randomly, without taking into account different exposure groups.

(3) Model selection

Two model selection methods were considered:

(i) The models with the best average performance over the five octave frequency bands was chosen. Therefore, for one particular type of prediction model, only one model was chosen.

(ii) Octave bands based model selection: The models was chosen according to the performance in each octave frequency band, the model with the best performance for one particular octave frequency band was chosen, as a result, there might be up to 5 different models chosen for one particular type of prediction model.

(4) Model structure design

(a) MLP neural network model selection

1. Preprocessing and postprocessing

Neural network training can be made more efficient if certain preprocessing steps are performed on the network inputs and outputs. It is useful to scale the inputs and outputs before training, such that they always fall within a specified range. A nonlinear tan-sigmoid was chosen as the activation function of the neural networks, which generates an output in the range of [-1,1], the preprocessing method that scales the inputs and outputs of the neural networks into the range [-1, 1] was deployed. It should be noted, whenever the trained network is used with new inputs, they should be preprocessed with the same minimum and maximums which were computed for the training set, and the outputs of the neural networks should be postprocessed to covert back to their original units.

2. Hidden layers

In our modeling efforts we tried MLP structures with one and two hidden layers. Table 5 shows the performance comparison of MLP with two structures.

Table 5 Percent of prediction accuracy for IHC loss using the MLP, partition method 1.

	Prediction Accuracy for IHC loss (percent)						
Frequency	0.5kHz	1kHz	2kHz	4kHz	8kHz	Average	No. of neuron @ each layer
MLP (1hid 1 output)	90.05	82.20	82.41	91.50	86.96	86.62	20
MLP (2hid 1 output)	92.23	70.41	82.19	95.44	88.40	85.73	20 30
MLP (2hid 3 outputs)	86.67	88.07	91.09	91.91	95.55	90.66	30 20
MLP (1hid 3 outputs)	**90.56**	**78.30**	**88.21**	**97.30**	**93.88**	**89.65**	**30**
	Prediction Accuracy for OHC loss (percent)						
Frequency	0.5kHz	1kHz	2kHz	4kHz	8kHz	Average	
MLP (1hid 1 output)	92.24	79.82	78.27	95.03	92.13	87.50	25
MLP (2hid 1 output)	90.60	94.62	82.94	94.41	89.45	90.40	10 20
MLP (2hid 3 outputs)	91.82	79.61	84.47	94.61	92.66	88.63	30 30
MLP (1hid 3 outputs)	**94.93**	**78.48**	**83.88**	**95.03**	**90.27**	**88.52**	**30**
	Prediction Accuracy for PTS (percent)						
Frequency	0.5kHz	1kHz	2kHz	4kHz	8kHz	Average	
MLP (1hid 1 output)	95.85	91.22	91.31	87.07	89.76	91.04	20
MLP (2hid 1 output)	91.82	87.29	88.94	93.81	93.49	91.07	30 20
MLP (2hid 3 outputs)	92.54	96.06	88.21	94.31	92.34	92.69	20 20
MLP (1hid 3 outputs)	**91.00**	**94.61**	**88.61**	**94.20**	**92.14**	**92.11**	**30**

It was found that the performance of the structure with two layers was not significantly better than the one with one layer, which means a single hidden layer is sufficient for a multilayer network to approximate any function of interest to any degree of accuracy, provided sufficiently many hidden units are available. Thus, one hidden layer neural network with three outputs of MLP was chosen as the basic models structure.

3. Initializing weights and bias

Before training a neural network, the weights and biases need to be initialized. The initialization methods were chosen depending on the structure of the network. For the layer with a linear transfer function, the weights are initialized to random values between -1 and 1. For the layer with a nonlinear transfer function, an initialization method based on the technique of Nguyen and Widrow (was used. It generates initial weight and bias values for a layer such that the active regions of the layer's neurons will be distributed roughly evenly over the input space. Comparing with the pure random weights, this technique has several advantages: a) few neurons are wasted, since the active regions of all the neurons are in the input space; b) training works faster, since each area of the input space has active neuron regions.

4. Training algorithm

The network was read for training after the initialization. The Levenberg-Marquardt algorithm (Hagan et al., 1996; Scales, 1985) was selected as the training algorithm for the proposed MLP network due to its fast convergence and accurate training ability for networks containing up to a few hundred weights. The detailed training algorithm is not given here, the interested readers may refer to the corresponding references.

5. Generalization

One of the problems that occur during neural network training is overfitting. The error on the training set is driven to a very small value, but when new data is presented to the network, the error is large. The network has memorized the training examples, but it has not learned to generalize to new situations. In order to improve generalization, an early stopping method was used. In this technique, the available data is divided into training, validation and testing sets. The training set was used to compute the gradient and updating the network weights and biases. The error on the validation set is monitored during the training process. The validation error will normally decrease during early phase of training, as does the training error, however, when the network begins to overfit the data, the error on the validation set will typically begin to rise. The training is stopped when the validation error increases for a specified number of iterations, and the weights and biases obtained at the minimum validation error are returned.

6. Complexity of network

Usually, the larger a network is used, the more complex the functions that the network can create. A smaller network may be less likely to learn the noises in the training data, and may generalize better to new data. To obtain a network with minimum size while maintaining good performance, the method of network growing was used. A network with small number of perceptrons is used first, and new perceptrons are added until the performance of the network deteriorates. The network with the best performance was chosen.

(b) RBF regression networks model selection

1. Preprocessing and postprocessing

The preprocessing and postprocessing of the inputs and output in the construction and testing of RBFNN are the same as the ones used in neural network.

2. Weights and other parameter setting

The weights of the RBF were determined according to the training data, as described in the RBFNN model structure section. The parameter SPREAD was used to calculate the value of the bias. The value of SPREAD should be large enough that neurons respond strongly to overlapping regions of the input space. This will make the network function smoother and results in better generalization for new input vectors occurring between input vectors used for constructing the network. The SPREAD is set through iteration: first setting a small value for SPREAD and then increasing the value by a step size in each iteration until the performance deteriorates.

(c) LS-SVM model selection

1. Preprocessing and postprocessing

The inputs and outputs of the LS-SVM model are normalized such that they have zero mean and unity standard deviation, and the outputs of the model are converted back to their original units when new input data is applied to the trained LSSVM model.

2. Parameter tuning

As an RBF kernel is selected, two parameters (γ, σ) need to be tuned: γ is the regulation parameter, determining the trade-off between the fitting error minimization and smoothness of the estimation function, and σ is the kernel function parameter. One way to infer the values of the two parameters is through Bayesian inference LS-SVM function estimator (regressor) with several levels of inference (Suykens et al., 2002), which takes probabilistic interpretations of the network outputs and

determines the tuning parameters (hyperparamters) automatically. Basically, the Bayesian inference has three levels of inference, the first level is used for predicting mean and error bars through probabilistic interpretation of the LS-SVM regressors. In level two, the hyperparameters (in this case, it is the regulation parameter γ) are determined and kernel parameters (in this case, it is the RBF kernel function parameter σ) are determined in level three. However, this method did not achieve the best performance after testing the models using current data. As a result, this method was not used for the final model selection. Another possible way was through iteration. Though the best performance could not be achieved through Bayesian inference, the tuning parameters obtained from it could be used as the reference values for other algorithms. Taking into account the results returned from Bayesian inference and the testing results, the regulation parameter γ was set to 10, and the RBF kernel function parameter σ was determined according to the structure and performance of the model.

V. Numerical Results

Part I: Complex noise induced hearing loss models

Total 322 animals exposed under 30 complex noise conditions were used to build the three statistical prediction models mentioned above. Since all exposures were 5-day continuous noise exposures, asymptotic threshold shift *ATS(f)* was used as an input instead of *TS(f)*.

(1) Energy only versus energy plus kurtosis

To demonstrate the value of kurtosis as a new effective metric for estimating NIHL from complex industrial noise environments, two inputs strategies for the three models were used as listed in Table I-1.

Table I-1 Energy only and energy plus kurtosis inputs

Inputs (independent variables)	Outputs (dependent variables)
Energy only: 1. Weighted energy, $E_w(t)$; 2. Weighted energy in filtered octave bands $E_w(f)$ at cf = 0.5, 1, 2, 4, 8 kHz; 3. Pre-exposure auditory evoked potential thresholds, $PRE_{EP}(f)$ at cf = 0.5, 1, 2, 4, 8 kHz	Indices of trauma to the auditory system (at specific center frequencies): 1. Noise-induced PTS, *PTS(f)* (dB) at cf = 0.5, 1, 2, 4, 8 kHz; 2. Outer hair cell loss, *OHC(f)*(%) at cf = 0.5, 1, 2, 4, 8 kHz; 3. Inner hair cell loss, *IHC(f)* (%)at cf = 0.5, 1, 2, 4, 8 kHz;
Energy plus kurtosis: 1. Weighted energy, $E_w(t)$; 2. Weighted energy in filtered octave bands $E_w(f)$ at cf = 0.5, 1, 2, 4, 8 kHz; 3. Kurtosis in time domain, $\beta(t)$; 4. Kurtosis in frequency domain $\beta(f)$ at cf = 0.5, 1, 2, 4, 8 kHz; 5. Pre-exposure auditory evoked potential thresholds, $PRE_{EP}(f)$ at cf = 0.5, 1, 2, 4, 8 kHz;	

The performance of three models for energy only and energy plus kurtosis is listed in Table I-2. We used the improvement in the percent of error rate to evaluate the improvement in the performance between algorithm 1 and algorithm 2 as described below:

$$PI = \frac{E_{A1} - E_{A2}}{E_{A1}} (\%) \tag{23}$$

where PI is the improvement in the percent of error rate, and E_{A1} and E_{A2} are the error rates from algorithm 1 and algorithm 2, respectively. For example: if the error rate from algorithm 1 is 0.1 and error rate from algorithm 2 is 0.06, the PI=40%, it can be said that the performance of algorithm 2 was improved by 40% compared to algorithm 1.

Table I-2(a1) Prediction accuracy in percent for IHC loss using three models and two partition methods.

Model \ Frequency	0.5kHz	1kHz	2kHz	4kHz	8kHz	Average	Partition method
MLP Energy only	83.50	82.08	78.16	88.07	64.82	79.33	1
MLP E plus β	84.34	84.26	89.02	92.97	92.77	88.67	1
MLP Energy only	90.63	85.31	75.63	82.81	62.19	79.31	2
MLP E plus β	98.44	78.13	82.50	87.81	90.31	87.44	2
RBF Energy only	83.12	83.42	82.50	79.09	73.19	80.26	1
RBF E plus β	92.96	90.46	91.61	88.92	89.96	90.78	1
RBF Energy only	82.50	84.38	80.31	82.19	72.50	80.38	2
RBF E plus β	93.44	88.13	94.06	90.94	89.69	91.25	2
SVM Energy only	83.02	78.36	78.87	80.12	74.31	78.94	1
SVM E plus β	87.99	85.19	86.43	90.16	90.47	88.05	1
SVM Energy only	82.81	80.00	76.56	80.63	75.94	79.19	2
SVM E plus β	91.25	84.38	86.25	93.44	92.50	89.56	2

Table I-2(a2) Performance improvement in percent for IHC loss (E plus β vs Energy only)

Model \ Frequency	0.5kHz	1kHz	2kHz	4kHz	8kHz	Average	Partition method
MLP	5.09	12.17	49.73	41.07	79.45	45.19	1
MLP	83.35	-48.88	28.19	29.09	74.37	39.29	2
RBF	58.29	42.46	52.06	47.01	62.55	53.29	1
RBF	62.51	24.01	69.83	49.13	62.51	55.40	2
SVM	29.27	31.56	35.78	50.50	62.90	43.26	1
SVM	49.10	21.90	41.34	66.13	68.83	49.83	2

Table I-2(a1) shows the prediction accuracy for IHC loss using three models and two partition methods. It is clear that if the kurtosis is used as an additional metric the average prediction accuracy could be as high as 91% using RBF model. Table I-2(a2) gives the performance improvement percent for IHC loss with energy only and with energy plus kurtosis. It shows that the model with energy plus kurtosis improved the prediction performance significantly. The average performance improvement percents range from 39% to 55%. The RBF model with energy plus kurtosis has the best average performance for IHC loss prediction. It is interesting to note that the prediction accuracy (or the error rate) at 8 kHz got the most improvement if the kurtosis metric was combined into the prediction models.

Table I-2(b) Prediction accuracy in percent for OHC loss using three models with different partitions.

Model \ Frequency	0.5kHz	1kHz	2kHz	4kHz	8kHz	Average	Partition method
MLP Energy only	85.73	84.70	73.40	84.78	79.21	81.56	1
MLP E plus β	97.61	76.23	81.78	89.65	83.04	85.66	1
MLP Energy only	77.50	74.37	68.13	82.81	60.94	72.75	2
MLP E plus β	93.75	79.38	83.75	85.63	87.81	86.06	2
RBF Energy only	85.70	80.54	76.30	78.77	67.39	77.74	1
RBF E plus β	94.81	91.61	94.82	95.13	86.54	92.59	1
RBF Energy only	83.44	79.69	75.63	76.88	68.13	76.75	2
RBF E plus β	93.44	87.81	91.88	94.38	80.00	89.50	2
SVM Energy only	84.46	78.80	78.26	76.82	67.90	77.25	1
SVM E plus β	94.61	90.90	89.55	92.14	88.42	91.12	1
SVM Energy only	84.38	77.50	77.81	75.94	64.06	75.94	2
SVM E plus β	94.69	90.00	90.31	92.19	90.62	91.56	2

Table I-2(b2) Performance improvement in percent for OHC loss (E plus β vs Energy only).

Model \ Frequency	0.5kHz	1kHz	2kHz	4kHz	8kHz	Average	Partition method
MLP	83.25	-55.36	31.50	32.00	18.42	22.23	1
MLP	72.22	19.55	49.01	16.40	68.79	48.84	2
RBF	63.71	56.89	78.14	77.06	58.72	66.71	1
RBF	60.39	39.98	66.68	75.69	37.25	54.84	2
SVM	65.32	57.08	51.93	66.09	63.93	60.97	1
SVM	66.01	55.56	56.33	67.54	73.90	64.92	2

Table I-2(b1) shows the prediction accuracy for OHC loss using three models with different partition methods. It is clear that if the kurtosis is used as an additional metric the average prediction accuracy could be as high as 92% using RBF model. Table I-2(b2) gives the performance improvement percent for OHC loss with energy only and with energy plus kurtosis. It shows that the model with energy plus kurtosis improved the prediction performance significantly. The average performance improvement percents range from 22% to 66%. Both RBF and SVM models with energy plus kurtosis have very good average performance for OHC loss prediction.

Table I-2(c) Prediction accuracy in percent for PTS using the three models with different partitions.

Frequency / Model	0.5kHz	1kHz	2kHz	4kHz	8kHz	Average	Partition method
MLP Energy only	82.42	92.24	73.72	86.55	75.78	82.14	1
MLP E plus β	94.21	83.86	91.20	88.92	88.82	89.40	1
MLP Energy only	75.94	86.88	78.13	86.25	67.50	78.94	2
MLP E plus β	88.75	92.50	91.25	95.00	92.19	91.94	2
RBF Energy only	87.27	87.06	81.68	78.87	69.26	80.83	1
RBF E plus β	90.17	93.99	93.69	94.30	89.44	92.32	1
RBF Energy only	88.44	86.25	84.38	83.13	74.38	83.31	2
RBF E plus β	94.69	96.56	95.63	93.13	85.00	93.00	2
SVM Energy only	84.48	88.94	80.13	82.82	71.12	81.50	1
SVM E plus β	93.17	93.27	88.40	90.58	91.10	91.30	1
SVM Energy only	86.25	91.25	80.63	81.25	71.25	82.13	2
SVM E plus β	95.63	95.00	89.06	89.38	86.56	91.13	2

Table I-2(c2) Performance improvement in percent for PTS (E plus β vs Energy only).

Frequency / Model	0.5kHz	1kHz	2kHz	4kHz	8kHz	Average	Partition method
MLP	67.06	-107.99	66.51	17.62	53.84	40.65	1
MLP	53.24	42.84	59.99	63.64	75.97	61.73	2
RBF	22.78	53.55	65.56	73.02	65.65	59.94	1
RBF	54.07	74.98	72.02	59.28	41.45	58.06	2
SVM	55.99	39.15	41.62	45.17	69.18	52.97	1
SVM	68.22	42.86	43.52	43.36	53.25	50.36	2

Table I-2(c1) shows the prediction accuracy for PTS using three models with two partition methods. It is clear that if the kurtosis is used as an additional metric the average prediction accuracy could be as high as 93% using RBF model. Table I-2(c2) gives the performance improvement percent for PTS with energy only and with energy plus kurtosis. It shows that the model with energy plus kurtosis improved the prediction performance significantly. The average performance improvement percents range from 40% to 61%. The RBF model with energy plus kurtosis has the best average performance for PTS prediction. As seen previously, the prediction accuracy (or the error rate) at 8 kHz improved the most if the kurtosis metric was entered into the prediction models.

Conclusion:

1. Energy alone is not a sufficient metric to predict complex noise induced hearing hazard. Kurtosis is a complementary metric. With the kurtosis metric performance of the prediction models is improved as much as 66%, a significant improvement.
2. While three models show good performance for IHC, OHC and PTS prediction, the RBF has the best average performance, the performance of the SVM model is quite close to the RBF and the MLP model is the weakest.

(2) ATS as one of the inputs to the prediction models

It is arguable whether TTS or ATS is a good indicator of PTS (Hamernik and Ahroon, 1998). For the 5-day continuous exposures only ATS was measured. To demonstrate the contribution of ATS to the performance of the prediction models, two sets of inputs were chosen to test the prediction models. One set includes all 8 possible variables listed in Table I-3 (denoted as 'All'), and the other set included all variables except ATS (denoted as "All but ATS"). The performance of the prediction models was evaluated in terms of the average percent predicted accuracy of IHC loss, OHC loss, PTS and change of DPOAE respectively, and is shown in Table I-4.

Table I-3: Input and output variables used in the models for complex noise prediction performance.

Inputs (independent variables)	Outputs (dependent variables)
Noise metrics: 1. Weighted energy, $E_w(t)$; 2. Kurtosis in time domain, $\beta(t)$; 3. Probability of a transient occurring, P; 4. Kurtosis in frequency domain $\beta(f)$ at cf = 0.5, 1, 2, 4, 8 kHz; 5. Weighted energy in filtered octave bands $E_w(f)$ at cf = 0.5, 1, 2, 4, 8 kHz; 6. The energy of background noise, $E_b(t)$; 7. Pre-exposure auditory evoked potential thresholds, $PRE_{EP}(f)$ at cf = 0.5, 1, 2, 4, 8 kHz; 8. Asymptotic threshold shift, $ATS(f)$ at cf = 0.5, 1, 2, 4, 8 kHz	Indices of trauma to the auditory system (at specific center frequencies): 1. Noise-induced PTS, $PTS(f)$ (dB) at cf = 0.5, 1, 2, 4, 8 kHz; 2. Outer hair cell loss, $OHC(f)$(%) at cf = 0.5, 1, 2, 4, 8 kHz; 3. Inner hair cell loss, $IHC(f)$ (%)at cf = 0.5, 1, 2, 4, 8 kHz;

Table I-4(a1) Comparison of prediction accuracy in percent for IHC loss using the three models with/without ATS input.

Model \ Frequency	0.5kHz	1kHz	2kHz	4kHz	8kHz	Average	Partition method
MLP All	88.82	82.40	88.19	82.11	95.24	87.35	1
MLP All but AST	90.56	78.30	88.21	97.30	93.88	89.65	1
MLP All	86.88	79.38	89.06	89.38	86.56	86.25	2
MLP All but AST	90.00	86.25	80.00	96.56	91.25	88.81	2
RBF All	95.24	89.02	90.36	90.69	88.71	90.81	1
RBF All but AST	95.86	91.61	92.55	87.68	91.10	91.76	1
RBF All	90.94	88.44	88.75	89.69	87.50	89.06	2
RBF All but AST	90.94	89.69	90.63	90.00	89.38	90.13	2
SVM All	87.36	84.36	86.02	91.10	92.66	88.30	1
SVM All but AST	89.64	86.65	88.19	91.83	93.28	89.92	1
SVM All	91.56	85.00	85.00	91.88	88.44	88.38	2
SVM All but AST	85.94	85.00	84.38	92.50	92.81	88.13	2

Table I-4(a2) Performance improvement in percent for IHC loss (All but ATS vs All).

Model \ Frequency	0.5kHz	1kHz	2kHz	4kHz	8kHz	Average	Partition method
MLP	15.56	-23.30	0.17	84.91	-28.57	18.18	1
MLP	23.78	33.32	-82.82	67.61	34.90	18.62	2
RBF	13.03	23.59	22.72	-32.33	21.17	10.34	1
RBF	0.00	10.81	16.71	3.01	15.04	9.78	2
SVM	18.04	14.64	15.52	8.20	8.45	13.85	1
SVM	-66.59	0.00	-4.13	7.64	37.80	-2.15	2

Table I-4(a1) shows the prediction accuracy for IHC loss using the three models with and without ATS. Table I-4(a2) gives the performance percent improvement for IHC loss with "All but ATS" and "All" input systems. As shown in the above tables in some frequency bands using the ATS as an additional input did yield better performance (such as the MLP model at 2 kHz with partition method 2), the average performance improvement for IHC loss prediction using "All but ATS" is better than that of using All, which means that the role of ATS in the IHC loss prediction models is not important. The RBF model with "All but ATS" has the best average performance for IHC loss prediction, though it only beat SVM and MLP models by 2~3%.

Table I-4(b1) Comparison of prediction accuracy in percent for OHC loss using the three models with/without ATS input.

Frequency / Model	0.5kHz	1kHz	2kHz	4kHz	8kHz	Average	Partition method
MLP All	88.11	81.68	76.94	81.69	91.64	84.01	1
MLP All but AST	94.93	78.48	83.88	95.03	90.27	88.52	1
MLP All	91.25	83.75	85.31	84.06	83.44	85.56	2
MLP All but AST	87.19	82.50	80.00	93.75	85.63	85.81	2
RBF All	95.77	89.76	93.48	94.11	84.57	91.54	1
RBF All but AST	96.37	90.99	95.44	93.79	86.25	92.69	2
RBF All	95.94	86.25	88.75	92.50	83.13	89.31	1
RBF All but AST	96.25	87.50	94.69	94.38	82.19	91.00	2
SVM All	93.28	89.22	86.64	87.79	84.47	88.28	1
SVM All but AST	95.03	90.48	92.86	91.00	88.51	91.57	1
SVM All	91.56	86.88	85.94	90.00	85.63	88.00	2
SVM All but AST	92.81	89.69	90.00	94.69	90.31	91.50	2

Table I-4(b2) Performance improvement in percent for OHC loss (All but ATS vs All).

Frequency / Model	0.5kHz	1kHz	2kHz	4kHz	8kHz	Average	Partition method
MLP	57.36	-17.47	30.10	72.86	-16.39	28.21	1
MLP	-46.40	-7.69	-36.15	60.79	13.22	1.73	2
RBF	14.18	12.01	30.06	-5.43	10.89	13.59	1
RBF	7.64	9.09	52.80	25.07	-5.57	15.81	2
SVM	26.04	11.69	46.56	26.29	26.01	28.07	1
SVM	14.81	21.42	28.88	46.90	32.57	29.17	2

Table I-4(b1) shows the prediction accuracy of OHC loss using the three models with and without ATS. Table I-4(b2) gives the performance percent improvement for OHC loss with "All but ATS" and "All" input systems. As shows in the above tables the performance percent improvement in Table -4(b2) is mixed with positive and negative changes in various frequency bands, the average performance improvement for OHC loss prediction using "All but ATS" is basically better than that of using "All" inputs, which means the role of ATS in the OHC loss prediction models is not important. The performance of the RBF and SVM models with "All but ATS" are very close, while the average performance of the MLP model is lower than the SVM and RBF models by 4% to 7%.

Table I-4(c1) Comparison of prediction accuracy in percent for PTS using the three models with/without ATS input.

Model \ Frequency	0.5kHz	1kHz	2kHz	4kHz	8kHz	Average	Partition method
MLP All	87.46	87.67	79.92	89.45	93.59	87.62	1
MLP All but AST	91.00	94.61	88.61	94.20	92.14	92.11	1
MLP All	90.00	79.38	90.94	88.44	88.75	87.50	2
MLP All but AST	89.38	95.00	80.94	91.88	90.00	89.44	2
RBF All	94.52	94.31	93.69	95.24	88.51	93.25	1
RBF All but AST	95.65	95.34	94.31	96.17	89.54	94.20	1
RBF All	94.69	90.94	91.25	95.63	88.75	92.25	2
RBF All but AST	96.25	92.81	92.50	96.88	82.81	92.25	2
SVM All	89.75	89.95	86.23	86.86	90.59	88.68	1
SVM All but AST	93.99	95.55	88.10	93.07	91.82	92.51	1
SVM All	90.00	88.75	86.25	90.31	85.63	88.19	2
SVM All but AST	95.00	98.13	87.19	91.88	88.75	92.19	2

Table I-4(c2) Performance improvement in percent for PTS (All but ATS vs All).

Model \ Frequency	0.5kHz	1kHz	2kHz	4kHz	8kHz	Average	Partition method
MLP	28.23	56.29	43.28	45.02	-22.62	36.27	1
MLP	-6.20	75.75	-110.38	29.76	11.11	15.52	2
RBF	20.62	18.10	9.83	19.54	8.96	14.07	1
RBF	29.38	20.64	14.29	28.60	-52.80	0.00	2
SVM	41.37	55.72	13.58	47.26	13.07	33.83	1
SVM	50.00	83.38	6.84	16.20	21.71	33.87	2

Table I-4(c1) shows the prediction accuracy for PTS using the three models with and without ATS. Table I-4(c2) gives the performance improvement percent for PTS with "All but ATS" and "All" input systems. As shown in the above tables in some frequency bands using the ATS as an additional input did yield better performance (such as the MLP model at 2 kHz with partition method 2), the average performance improvement for IHC loss prediction using "All but ATS" is better than that of using All, which means that the role of ATS in the PTS prediction models is not important. The performance of the models was close while the RBF model is a little bit better than the other two models.

Conclusion: The inclusion of ATS in the models does not improve the performance of the prediction models. The average performance of the three models without an ATS input, either by partition method 1 or 2, is better than that of the models with ATS input. Thus ATS will not be used as an input for the subsequent prediction models.

(3) Wide frequency and specific frequency model comparison

Since thresholds and otoacoustic emissions are measured at multiple frequencies and OHC/IHC loss is evaluated at multiple locations that are eventually transformed to corresponding frequencies (Eldredge et al., 1981), NIHL must be evaluated in a frequency specific manner. This makes it necessary to account for a possible correlation between contiguous frequency bands. Two frequency specific prediction models were considered:

(i) Specific frequency model (SF model): Five frequencies are considered (cf = 0.5, 1, 2, 4, 8 kHz). That is, a prediction model was built for each specified frequency. Hence, there will be five prediction models each one good only for the specified frequency.

(ii) Wide band frequency model (WF model): In the SF model the correlation between different frequency bands, especially between contiguous frequency bands is not considered. In the WF prediction model contiguous frequency band information on either upper or lower side(s) of a specified frequency band was considered as additional input(s) for the models. Two WF methods were used. One is both-side WF, i.e. both upper and lower sides of a specific frequency band are used as additional inputs. For example, if 1 kHz is selected for an estimate of its indices of trauma in the input layer, then the frequency kurtosis, energy spectra, initial AEP thresholds, etc. at cf = 0.5 and 2 kHz will also be input for both-side WF model. At extreme points (i.e. 0.5 kHz and 8 kHz) only the right or left frequency band will be added to the input layer. The other is upper-side WF, i.e. only upper side of a specific frequency band is used as an additional input. For instance, if 1 kHz is selected for an estimate of its indices of trauma in the input layer, then the frequency kurtosis, energy spectra, initial AEP thresholds, etc. at cf = 2 kHz will also be input. At extreme point (i.e. 8 kHz) there is no upper side input.

Table I-5(a1) Percent prediction accuracy for IHC loss using the three models (SF vs. WF).

Frequency / Model	0.5kHz	1kHz	2kHz	4kHz	8kHz	Average	Partition method
MLP SF	90.56	78.3	88.21	97.3	93.88	89.65	1
MLP both-side WF	86.65	82.74	90.67	84.49	87.79	86.47	1
MLP upper-side WF	88.41	81.48	92.55	86.64	90.1	87.84	1
MLP SF	90	86.25	80	96.56	91.25	88.81	2
MLP both-side WF	90.94	71.25	84.38	89.69	91.56	85.56	2
MLP upper-side WF	91.56	86.87	82.19	87.5	88.44	87.31	2
RBF SF	95.86	91.61	92.55	87.68	91.10	91.76	1
RBF both-side WF	91.21	91.19	91.61	92.55	91.81	91.67	1
RBF upper-side WF	92.45	87.97	91.82	92.35	91.4	91.2	1
RBF SF	90.94	89.69	90.63	90.00	89.38	90.13	2
RBF both-side WF	93.75	94.06	90.94	91.56	89.69	92.00	2
RBF upper-side WF	95.63	87.5	91.56	93.44	89.38	91.5	2
SVM SF	89.64	86.65	88.19	91.83	93.28	89.92	1
SVM both-side WF	86.34	83.74	87.26	89.86	91.81	87.80	1
SVM upper-side WF	89.12	84.47	86.84	89.66	91.71	88.36	1
SVM SF	85.94	85.00	84.38	92.50	92.81	88.13	2
SVM both-side WF	86.25	82.19	85.94	89.38	90.63	86.88	2
SVM upper-side WF	90.31	82.5	89.69	93.75	92.81	89.81	2

Table I-5(a2) Change in percent of the prediction error rate for IHC loss using the three methods (SF vs Both-side WF).

Frequency / Model	0.5kHz	1kHz	2kHz	4kHz	8kHz	Average	Partition method
MLP	29.29	-25.72	-26.37	82.59	49.88	23.50	1
MLP	-10.38	52.17	-28.04	66.63	-3.67	22.51	2
RBF	52.90	4.77	11.20	-65.37	-8.67	1.08	1
RBF	-44.96	-73.57	-3.42	-18.48	-3.01	-23.38	2
SVM	24.16	17.90	7.30	19.43	17.95	17.38	1
SVM	-2.25	15.78	-11.10	29.38	23.27	9.53	2

Table I-5(a3) Change in percent of the prediction error rate for IHC loss using the three methods (SF vs Upper-side WF).

Frequency / Model	0.5kHz	1kHz	2kHz	4kHz	8kHz	Average	Partition method
MLP	18.55	-17.17	-58.26	79.79	38.18	14.88	1
MLP	-18.48	-4.72	-12.30	72.48	24.31	11.82	2
RBF	45.17	30.26	8.92	-61.05	-3.49	6.36	1
RBF	-107.32	17.52	-11.02	-52.44	0.00	-16.12	2
SVM	4.78	14.04	10.26	20.99	18.94	13.40	1
SVM	-45.10	14.29	-51.50	-20.00	0.00	-16.49	2

Table I-5(a4) Change in percent of the prediction error rate for IHC loss using the three methods (Both-side WF vs Upper-side WF).

Frequency / Model	0.5kHz	1kHz	2kHz	4kHz	8kHz	Average	Partition method
MLP	-15.19	6.80	-25.23	-16.09	-23.33	-11.27	1
MLP	-7.35	-118.96	12.30	17.52	26.99	-13.79	2
RBF	-16.42	26.77	-2.57	2.61	4.77	5.34	1
RBF	-43.02	52.48	-7.35	-28.66	2.92	5.88	2
SVM	-25.55	-4.70	3.19	1.93	1.21	-4.81	1
SVM	-41.90	-1.77	-36.37	-69.92	-30.32	-28.75	2

Table I-5(a1) presents the percent of prediction accuracy for IHC loss for the three models. Table I-5(a2)-(a4) give the percentage change in prediction error rate for IHC loss using SF vs. Both-side WF, SF vs. Upper-side WF, and Both-side WF vs. Upper-side WF, respectively. The overall performance of the SF model with partition method 1 is always better than that of the WF model. In partition method 2 the average performance of the RBF and SVM models using the SF model got worse in comparison with the WF model. For the two WF methods, the upper-side WF seems better than the both-side WF model. The performance difference between SF and WF is not significant in the IHC loss prediction.

Table I-5(b1) Percent prediction accuracy for OHC loss using the three models (SF vs. WF).

Frequency / Model	0.5kHz	1kHz	2kHz	4kHz	8kHz	Average	Partition method
MLP SF	94.93	78.48	83.88	95.03	90.27	88.52	1
MLP both-side WF	87.6	79.19	82.31	92.87	90.27	86.45	1
MLP upper-side WF	94.74	81.82	79.72	91.1	89.44	87.36	1
MLP SF	87.19	82.5	80	93.75	85.63	85.81	2
MLP both-side WF	86.88	86.25	87.5	84.69	87.5	86.56	2
MLP upper-side WF	93.12	84.69	84.06	85	94.38	88.25	2
RBF SF	96.37	90.99	95.44	93.79	86.25	92.69	1
RBF both-side WF	93.79	91.41	94.21	94.10	90.98	92.90	1
RBF upper-side WF	95.13	91.31	92.34	91.93	91.19	92.38	1
RBF SF	96.25	87.50	94.69	94.38	82.19	91.00	2
RBF both-side WF	91.88	90.31	94.06	91.56	87.81	91.13	2
RBF upper-side WF	91.88	86.25	92.81	94.69	93.44	91.81	2
SVM SF	95.03	90.48	92.86	91.00	88.51	91.57	1
SVM both-side WF	94.62	90.06	89.14	90.99	92.86	91.53	1
SVM upper-side WF	96.37	91.4	91.93	89.86	91.51	92.22	1
SVM SF	92.81	89.69	90.00	94.69	90.31	91.50	2
SVM both-side WF	95.00	87.50	86.88	82.81	89.68	88.38	2
SVM upper-side WF	94.06	92.5	89.69	88.75	90.63	91.13	2

Table I-5(b2) Change of prediction error rate for OHC loss using the three methods (SF vs Both-side WF).

Frequency / Model	0.5kHz	1kHz	2kHz	4kHz	8kHz	Average	Partition method
MLP	59.11	-3.41	8.88	30.29	0.00	15.28	1
MLP	2.36	-27.27	-60.00	59.18	-14.96	-5.58	2
RBF	41.55	-4.89	21.24	-5.25	-52.44	-2.96	1
RBF	53.82	-29.00	10.61	33.41	-46.10	-1.47	2
SVM	7.62	4.23	34.25	0.11	-60.92	0.47	1
SVM	-43.80	17.52	23.78	69.11	6.10	26.85	2

Table I-5(b3) Change of prediction error rate for OHC loss using the three methods (SF vs Upper-side WF).

Frequency / Model	0.5kHz	1kHz	2kHz	4kHz	8kHz	Average	Partition method
MLP	3.61	-18.37	20.51	44.16	7.86	9.18	1
MLP	-86.19	-14.30	-25.47	58.33	-155.69	-20.77	2
RBF	25.46	-3.68	40.47	23.05	-56.07	4.07	1
RBF	53.82	9.09	26.15	-5.84	-171.49	-9.89	2
SVM	-36.91	-10.70	11.52	11.24	-35.34	-8.35	1
SVM	-21.04	-37.47	3.01	52.80	-3.42	4.17	2

Table I-5(b4) Change of prediction error rate for OHC loss using the three methods (Both-side WF vs Upper-side WF).

Model \ Frequency	0.5kHz	1kHz	2kHz	4kHz	8kHz	Average	Partition method
MLP	-135.74	-14.47	12.77	19.89	7.86	-7.20	1
MLP	-90.70	10.19	21.58	-2.07	-122.42	-14.38	2
RBF	-27.52	1.15	24.41	26.89	-2.38	6.82	1
RBF	0.00	29.53	17.39	-58.95	-85.82	-8.30	2
SVM	-48.21	-15.58	-34.57	11.14	15.90	-8.87	1
SVM	15.82	-66.67	-27.26	-52.80	-10.14	-31.00	2

Table I-5(b1) presents the percent prediction accuracy for OHC loss for the three models. Table I-5(b2)-(b4) give the percentage change in the prediction error rate for OHC loss using SF vs. Both-side WF, SF vs. Upper-side WF, and Both-side WF vs. Upper-side WF, respectively. The overall performance using the SF and WF models is mixed in the OHC loss prediction. There is no significant difference in prediction using either the SF model or the WF model.

Table I-5(c1) Percent prediction accuracy for PTS loss using the three models (WF vs. SF).

Model \ Frequency	0.5kHz	1kHz	2kHz	4kHz	8kHz	Average	Partition method
MLP SF	91	94.61	88.61	94.2	92.14	92.11	1
MLP Both-side WF	88.84	91.72	91.91	88.93	94.21	91.12	1
MLP Upper-side WF	97.09	90.93	86.44	88.2	96.05	91.74	1
MLP SF	89.38	95	80.94	91.88	90	89.44	2
MLP Both-side WF	88.75	90.63	89.69	86.87	92.5	89.69	2
MLP Upper-side WF	85.94	93.13	88.75	97.81	92.81	91.69	2
RBF SF	95.65	95.34	94.31	96.17	89.54	94.20	1
RBF Both-side WF	97.41	96.90	96.07	95.96	95.02	96.27	1
RBF Upper-side WF	93.37	95.44	95.75	95.55	95.75	95.17	1
RBF SF	96.25	92.81	92.50	96.88	82.81	92.25	2
RBF Both-side WF	96.25	95.63	96.56	93.44	93.44	95.06	2
RBF Upper-side WF	95	96.25	94.06	95	92.5	94.56	2
SVM SF	93.99	95.55	88.10	93.07	91.82	92.51	1
SVM Both-side WF	96.17	94.41	91.20	94.62	95.34	94.35	1
SVM Upper-side WF	93.89	95.86	91.93	94.21	95.34	94.25	1
SVM SF	95.00	98.13	87.19	91.88	88.75	92.19	2
SVM Both-side WF	93.75	90.94	92.19	93.75	94.69	93.06	2
SVM Upper-side WF	95.31	97.5	95	95.31	96.56	95.94	2

Table I-5(c2) Change of prediction error rate for PTS using the three methods (SF vs Both-side WF).

Model \ Frequency	0.5kHz	1kHz	2kHz	4kHz	8kHz	Average	Partition method
MLP	19.35	34.90	-40.79	47.61	-35.75	11.15	1
MLP	5.60	46.64	-84.87	38.16	-33.33	-2.42	2
RBF	-67.95	-50.32	-44.78	5.20	-110.04	-55.50	1
RBF	0.00	-64.53	-118.02	52.44	-162.04	-56.88	2
SVM	-56.92	20.39	-35.23	-28.81	-75.54	-32.57	1
SVM	20.00	79.36	-64.02	-29.92	-111.86	-12.54	2

Table I-5(c3) Change of prediction error rate for PTS using the three methods (SF vs upper-side WF).

Model \ Frequency	0.5kHz	1kHz	2kHz	4kHz	8kHz	Average	Partition method
MLP	-209.28	40.57	16.00	50.85	-98.99	4.48	1
MLP	24.47	27.22	-69.42	-270.78	-39.08	-27.08	2
RBF	34.39	-2.19	-33.88	13.93	-146.12	-20.08	1
RBF	25.00	-91.73	-26.26	37.60	-129.20	-42.46	2
SVM	1.64	-7.49	-47.46	-19.69	-75.54	-30.26	1
SVM	-6.61	25.20	-156.20	-73.13	-227.03	-92.36	2

Table I-5(c4) Change of prediction error rate for PTS using the three methods (both-side WF vs upper-side WF).

Model \ Frequency	0.5kHz	1kHz	2kHz	4kHz	8kHz	Average	Partition method
MLP	-283.51	8.71	40.34	6.19	-46.58	-7.51	1
MLP	19.99	-36.39	8.36	-499.54	-4.31	-24.07	2
RBF	60.94	32.02	7.53	9.21	-17.18	22.77	1
RBF	25.00	-16.53	42.09	-31.20	12.53	9.19	2
SVM	37.32	-35.02	-9.05	7.08	0.00	1.74	1
SVM	-33.26	-262.40	-56.20	-33.26	-54.36	-70.94	2

Table I-5(c1) presents the percent prediction accuracy for PTS using the three models. Table I-5(c2)-(c4) illustrate the percentage change in the prediction error rate for PTS using SF vs. Both-side WF, SF vs. Upper-side WF, and Both-side WF vs. Upper-side WF, respectively. In the case of PTS prediction the performance of the models with the WF model is significantly better than that of the SF model. The prediction error rates decreased from 2% to 57% for the three models using both-side WF model, and 20% to 92% using upper-side WF model.

Conclusion: There is not a significant difference between the SF and WF methods in the prediction of IHC and OHC loss. However, in the case of PTS prediction, the performance using both WF methods is significantly better than that of the SF method. The prediction error rate could be decreased as much as 92% using the upper-side WF. The results suggest that a WF prediction model could yield additional information for obtaining higher prediction accuracy. Since it is hard to say which of the two WF methods is better, a upper-side WF model was selected for its simpler structure in comparison to the both-side WF model.

(4) Complementary elements for kurtosis

Kurtosis is not unique. There are several factors that influence kurtosis, such as probability (P) of a transient occurring and the energy of the background noise (E_b). These two factors and their effects on prediction models are discussed in this section. The input and output variables are same as in Table I-3 except for the ATS input.

Table I-6(a1) Percent prediction accuracy for IHC loss using the three models with/without the kurtosis complementary elements.

Frequency / Model	0.5kHz	1kHz	2kHz	4kHz	8kHz	Average	Partition method
MLP	90.56	78.30	88.21	97.30	93.88	89.65	1
MLP no *Eb* & *P*	84.34	84.26	89.02	92.97	92.77	88.67	1
MLP	90.00	86.25	80.00	96.56	91.25	88.81	2
MLP no *Eb* & *P*	98.44	78.13	82.50	87.81	90.31	87.44	2
RBF	95.86	91.61	92.55	87.68	91.10	91.76	1
RBF no *Eb* & *P*	92.96	90.46	91.61	88.92	89.96	90.78	1
RBF	90.94	89.69	90.63	90.00	89.38	90.13	2
RBF no *Eb* & *P*	93.44	88.13	94.06	90.94	89.69	91.25	2
SVM	89.64	86.65	88.19	91.83	93.28	89.92	1
SVM no *Eb* & *P*	87.99	85.19	86.43	90.16	90.47	88.05	1
RBF	90.94	89.69	90.63	90.00	89.38	90.13	2
RBF no *Eb* & *P*	93.44	88.13	94.06	90.94	89.69	91.25	2

Table I-6(a2) Improvement in the percent error rate for the prediction of IHC loss using the three models (all vs no *Eb* & *P*).

Frequency / Model	0.5kHz	1kHz	2kHz	4kHz	8kHz	Average	Partition method
MLP	39.72	-37.87	-7.38	61.59	15.35	8.65	1
MLP	-541.03	37.13	-14.29	71.78	9.70	10.91	2
RBF	41.19	12.05	11.20	-11.19	11.35	10.63	1
RBF	-38.11	13.14	-57.74	-10.38	-3.01	-12.80	2
SVM	13.74	9.86	12.97	16.97	29.49	15.65	1
SVM	-38.11	13.14	-57.74	-10.38	-3.01	-12.80	2

Table I-6(a1) presents the percent prediction accuracy for IHC loss using the three models with/without *Eb* & *P*. Table I-6(a2) illustrates the percentage change in the prediction error rate for IHC loss. In the three models the average error rates all decreased using partition method 1 (the improvement rates are in the range 8% to 15%), while the error rates are mixed in the models using partition 2 (from -12% to 10%).

Table I-6(b1) Percent prediction accuracy for OHC loss using the three models with/without the kurtosis complementary elements.

Frequency / Model	0.5kHz	1kHz	2kHz	4kHz	8kHz	Average	Partition method
MLP	94.93	78.48	83.88	95.03	90.27	88.52	1
MLP no *Eb* & *P*	97.61	76.23	81.78	89.65	83.04	85.66	1
MLP	87.19	82.50	80.00	93.75	85.63	85.81	2
MLP no *Eb* & *P*	93.75	79.38	83.75	85.63	87.81	86.06	2
RBF	96.37	90.99	95.44	93.79	86.25	92.69	1
RBF no *Eb* & *P*	94.81	91.61	94.82	95.13	86.54	92.59	1
RBF	96.25	87.50	94.69	94.38	82.19	91.00	2
RBF no *Eb* & *P*	93.44	87.81	91.88	94.38	80.00	89.50	2
SVM	95.03	90.48	92.86	91.00	88.51	91.57	1
SVM no *Eb* & *P*	94.61	90.90	89.55	92.14	88.42	91.12	1
RBF	92.81	89.69	90.00	94.69	90.31	91.50	2
RBF no *Eb* & *P*	94.69	90.00	90.31	92.19	90.62	91.56	2

Table I-6(b2) Improvement in the percent error rate for the prediction of OHC loss using the three models (all vs no *Eb* & *P*).

Frequency / Model	0.5kHz	1kHz	2kHz	4kHz	8kHz	Average	Partition method
MLP	-112.13	9.47	11.53	51.98	42.63	19.94	1
MLP	-104.96	15.13	-23.08	56.51	-17.88	-1.79	2
RBF	30.06	-7.39	11.97	-27.52	-2.15	1.35	1
RBF	42.84	-2.54	34.61	0.00	10.95	14.29	2
SVM	7.79	-4.62	31.67	-14.50	0.78	5.07	1
SVM	-35.40	-3.10	-3.20	32.01	-3.30	-0.71	2

Table I-6(b1) presents the percent prediction accuracy of OHC loss for three models with/without *Eb* & *P*. Table I-6(b2) illustrates the percentage change in the prediction error rate for IHC loss. In the three models the average error rates all decreased using partition method 1 (the improvement rates are in the range 1% to 20%), while the error rates are mixed in the models using partition 2 (from -2% to 14%).

Table I-6(c1) Percent prediction accuracy for PTS using the three models with/without the kurtosis complementary element.

Model \ Frequency	0.5kHz	1kHz	2kHz	4kHz	8kHz	Average	Partition method
MLP	91.00	94.61	88.61	94.20	92.14	92.11	1
MLP no *Eb* & *P*	94.21	83.86	91.20	88.92	88.82	89.40	1
MLP	89.38	95.00	80.94	91.88	90.00	89.44	2
MLP no *Eb* & *P*	88.75	92.50	91.25	95.00	92.19	91.94	2
RBF	95.65	95.34	94.31	96.17	89.54	94.20	1
RBF no *Eb* & *P*	90.17	93.99	93.69	94.30	89.44	92.32	1
RBF	96.25	92.81	92.50	96.88	82.81	92.25	2
RBF no *Eb* & *P*	94.69	96.56	95.63	93.13	85.00	93.00	2
SVM	93.99	95.55	88.10	93.07	91.82	92.51	1
SVM no *Eb* & *P*	93.17	93.27	88.40	90.58	91.10	91.30	1
RBF	95.00	98.13	87.19	91.88	88.75	92.19	2
RBF no *Eb* & *P*	95.63	95.00	89.06	89.38	86.56	91.13	2

Table I-6(c2) Improvement in the percent error rate for the prediction of PTS using the three models (all vs no *Eb* & *P*).

Model \ Frequency	0.5kHz	1kHz	2kHz	4kHz	8kHz	Average	Partition method
MLP	-55.44	66.60	-29.43	47.65	29.70	25.57	1
MLP	5.60	33.33	-117.83	-62.40	-28.04	-31.02	2
RBF	55.75	22.46	9.83	32.81	0.95	24.48	1
RBF	29.38	-109.01	-71.62	54.59	-14.60	-10.71	2
SVM	12.01	33.88	-2.59	26.43	8.09	13.91	1
SVM	-14.42	62.60	-17.09	23.54	16.29	11.95	2

Table I-6(c1) presents the percent prediction accuracy for PTS for three models with/without *Eb* & *P*. Table I-6(c2) illustrates the percentage change in the prediction error rate for PTS. In the three models the average error rates all decreased using partition method 1 (the improvement rates are in the range of 14% to 25%), while the error rates are mixed in the models using partition 2 (from -31% to 12%).

Conclusion: The average improvement error rates in partition 1 are all positive, which suggests *Eb* and *P* are useful input for the prediction models. However, the improvement indexes were mixed in partition 2. The effect of *Eb* and *P* on prediction accuracy could not be neglected.

(5) Effects of the non frequency specific parameters $Ew(t)$, $\beta(t)$, Probability P, and $Eb(t)$

This section will check if frequency specific (octave band only, OB only) information alone is sufficient to predict NIHL at specific frequencies. Two input-output systems were checked as below:

Table I-7-1 Entire input-output system.

Inputs (independent variables)	Outputs (dependent variables)
Noise metrics: 1. Weighted energy, $E_w(t)$; 2. Kurtosis in time domain, $\beta(t)$; 3. Probability of a transient occurring in impulse/impact noise, P; 4. Kurtosis in frequency domain $\beta(f)$ at cf = 0.5, 1, 2, 4, 8 kHz; 5. Weighted energy in filtered octave bands $E_w(f)$ at cf = 0.5, 1, 2, 4, 8 kHz; 6. The energy of background noise, $E_b(t)$; 7. Pre-exposure auditory evoked potential thresholds, $PRE_{EP}(f)$ at cf = 0.5, 1, 2, 4, 8 kHz;	Indices of trauma to the auditory system (at specific center frequencies): 1. Noise-induced PTS, $PTS(f)$ (dB) at cf = 0.5, 1, 2, 4, 8 kHz; 2. Outer hair cell loss, $OHC(f)$(%) at cf = 0.5, 1, 2, 4, 8 kHz; 3. Inner hair cell loss, $IHC(f)$ (%)at cf = 0.5, 1, 2, 4, 8 kHz;

Table I-7-2 Octave band (OB) only input-output system.

Inputs (independent variables)	Outputs (dependent variables)
Noise metrics: 1. Kurtosis in frequency domain $\beta(f)$ at cf = 0.5, 1, 2, 4, 8 kHz; 2. Weighted energy in filtered octave bands $E_w(f)$ at cf = 0.5, 1, 2, 4, 8 kHz; 3. Pre-exposure auditory evoked potential thresholds, $PRE_{EP}(f)$ at cf = 0.5, 1, 2, 4, 8 kHz;	Indices of trauma to the auditory system (at specific center frequencies): 1. Noise-induced PTS, $PTS(f)$ (dB) at cf = 0.5, 1, 2, 4, 8 kHz; 2. Outer hair cell loss, $OHC(f)$(%) at cf = 0.5, 1, 2, 4, 8 kHz; 3. Inner hair cell loss, $IHC(f)$ (%)at cf = 0.5, 1, 2, 4, 8 kHz;

Table I-7(a1) Percent prediction accuracy for IHC loss using the three models (OB only vs. Entire).

Frequency / Model	0.5kHz	1kHz	2kHz	4kHz	8kHz	Average	Partition method
MLP	90.56	78.30	88.21	97.30	93.88	89.65	1
MLP OB only	77.83	82.58	79.90	85.52	91.82	83.53	1
MLP	90.00	86.25	80.00	96.56	91.25	88.81	2
MLP OB only	80.31	75.94	80.31	96.56	84.69	83.56	2
RBF	95.86	91.61	92.55	87.68	91.10	91.76	1
RBF OB only	88.50	83.32	90.25	87.99	83.74	86.76	1
RBF	90.94	89.69	90.63	90.00	89.38	90.13	2
RBF OB only	83.44	77.81	89.06	90.31	87.19	85.56	2
SVM	89.64	86.65	88.19	91.83	93.28	89.92	1
SVM OB only	77.83	80.21	82.50	88.62	84.78	82.79	1
SVM	85.94	85.00	84.38	92.50	92.81	88.13	2
SVM OB only	82.19	81.88	82.81	81.88	82.50	82.25	2

Table I-7(a2) Improvement in the percent error rate for the prediction of IHC loss using the three models (Entire vs OB only).

Frequency / Model	0.5kHz	1kHz	2kHz	4kHz	8kHz	Average	Partition method
MLP	57.42	-24.57	41.34	81.35	25.18	37.16	1
MLP	49.21	42.85	-1.57	0.00	42.85	31.93	2
RBF	64.00	49.70	23.59	-2.58	45.26	37.76	1
RBF	45.29	53.54	14.35	-3.20	17.10	31.65	2
SVM	53.27	32.54	32.51	28.21	55.85	41.43	1
SVM	21.06	17.22	9.13	58.61	58.91	33.13	2

Table I-7(a1) presents the percent prediction accuracy for IHC loss using the three models with OB only or whole variables. Table I-7(a2) illustrates the percentage change in the prediction error rate for IHC loss using OB only vs. whole variables. The prediction error rates decreased at least 31% for the three models using whole input method that means the models using OB only are not good enough for IHC loss prediction.

Table I-7(b1) Percent prediction accuracy for IHC loss using the three models (OB only vs. Entire).

Model \ Frequency	0.5kHz	1kHz	2kHz	4kHz	8kHz	Average	Partition method
MLP	94.93	78.48	83.88	95.03	90.27	88.52	1
MLP OB only	91.52	70.08	71.32	82.94	80.13	79.20	1
MLP	87.19	82.50	80.00	93.75	85.63	85.81	2
MLP OB only	90.31	76.25	82.81	92.50	81.25	84.63	2
RBF	96.37	90.99	95.44	93.79	86.25	92.69	1
RBF OB only	84.46	78.88	86.75	94.93	78.78	84.76	1
RBF	96.25	87.50	94.69	94.38	82.19	91.00	2
RBF OB only	84.38	78.44	89.69	93.13	75.31	84.19	2
SVM	95.03	90.48	92.86	91.00	88.51	91.57	1
SVM OB only	83.63	77.12	76.60	85.61	79.10	80.41	1
SVM	92.81	89.69	90.00	94.69	90.31	91.50	2
SVM OB only	85.31	75.31	73.13	90.63	79.38	80.75	2

Table I-7(b2) Improvement in the percent error rate for the prediction of IHC loss using the three models (Entire vs OB only).

Model \ Frequency	0.5kHz	1kHz	2kHz	4kHz	8kHz	Average	Partition method
MLP	40.21	28.07	43.79	70.87	51.03	44.81	1
MLP	-32.20	26.32	-16.35	16.67	23.36	7.68	2
RBF	76.64	57.34	65.58	-22.49	35.20	52.03	1
RBF	75.99	42.02	48.50	18.20	27.87	43.07	2
SVM	69.64	58.39	69.49	37.46	45.02	56.97	1
SVM	51.06	58.24	62.78	43.33	53.01	55.84	2

Table I-7(b1) presents the percent prediction accuracy for OHC loss using the three models with OB only or whole variables. Table I-7(b2) illustrates the percentage change in the prediction error rate for OHC loss using OB only or whole variables. The prediction error rates were highly improved for the three models using whole variables that means the models using OB only are not good enough for OHC loss prediction.

Table I-7(c) Percent prediction accuracy for PTS using the three models (OB only vs. Entire).

Model \ Frequency	0.5kHz	1kHz	2kHz	4kHz	8kHz	Average	Partition method
MLP	91.00	94.61	88.61	94.20	92.14	92.11	1
MLP OB only	83.86	85.92	82.20	87.89	87.07	85.39	1
MLP	89.38	95.00	80.94	91.88	90.00	89.44	2
MLP OB only	83.44	87.19	92.19	89.06	90.94	88.56	2
RBF	95.65	95.34	94.31	96.17	89.54	94.20	1
RBF OB only	82.60	86.32	88.20	91.09	87.06	87.06	1
RBF	96.25	92.81	92.50	96.88	82.81	92.25	2
RBF OB only	86.25	82.81	89.38	87.50	89.06	87.00	2
SVM	93.99	95.55	88.10	93.07	91.82	92.51	1
SVM OB only	79.19	87.36	84.68	86.64	82.82	84.14	1
SVM	95.00	98.13	87.19	91.88	88.75	92.19	2
SVM OB only	78.13	87.81	83.13	86.25	78.44	82.75	2

Table I-7(c2) Improvement in the percent error rate for the prediction of PTS using the three models (Entire vs OB only).

Model \ Frequency	0.5kHz	1kHz	2kHz	4kHz	8kHz	Average	Partition method
MLP	44.24	61.72	36.01	52.11	39.21	46.00	1
MLP	35.87	60.97	-144.05	25.78	-10.38	7.69	2
RBF	75.00	65.94	51.78	57.01	19.17	55.18	1
RBF	72.73	58.17	29.38	75.04	-57.13	40.38	2
SVM	71.12	64.79	22.32	48.13	52.39	52.77	1
SVM	77.14	84.66	24.07	40.95	47.82	54.72	2

Table I-7(c1) presents the percent prediction accuracy for PTS using the three models with OB only or whole variables. Table I-7(c2) illustrates the percentage change in the prediction error rate for PTS using OB only or whole variables. The prediction error rates were highly improved for the three models using whole variables that means the models using OB only are not good enough for PTS prediction.

Conclusion: Although the percent prediction accuracy could reach as high as 88% using OB only variables, the performance of prediction models using the entire variable set was much better. In most cases using all variables can get 30%~50% improved error rates in comparison with OB only models.

(6) Best model selection

There are two ways to select the best prediction model: One is to select the best model according to the best average prediction rate (Overall), and the other one is to pick up the best model based on the best performance of each band (Band based). Table I-8(a1) and (a2) present the best IHC loss prediction models selected using Overall and Band-based methods, Table I-8(b1) and (b2) present the best OHC loss prediction models selected using Overall and Band-based, and Table I-8(c1) and (c2) present the best PTS prediction models selected using Overall and Band-based, respectively.

Table I-8(a1) Percent prediction accuracy for IHC loss using the three models.

Frequency / Model	0.5kHz	1kHz	2kHz	4kHz	8kHz	Average	Partition method
MLP	90.56	78.30	88.21	97.30	93.88	89.65	1
MLP Band Based	90.56	89.14	91.20	97.30	93.88	92.41	1
MLP	90.00	86.25	80.00	96.56	91.25	88.81	2
MLP Band Based	90.00	87.19	90.63	96.56	91.25	91.13	2
RBF	95.86	91.61	92.55	87.68	91.10	91.76	1
RBF Band Based	95.86	91.61	92.55	91.31	91.10	92.48	1
RBF	90.94	89.69	90.63	90.00	89.38	90.13	2
RBF Band Based	97.50	89.69	91.25	90.00	90.94	91.88	2
SVM	89.64	86.65	88.19	91.83	93.28	89.92	1
SVM Band Based	89.64	87.58	88.81	91.83	93.28	90.23	1
SVM	85.94	85.00	84.38	92.50	92.81	88.13	2
SVM Band Based	90.63	85.00	85.97	92.50	92.81	89.38	2

Table I-8(a2) Improvement in the percent error rate for the prediction of IHC loss using the three models (Band based vs Overall).

Frequency / Model	0.5kHz	1kHz	2kHz	4kHz	8kHz	Average	Partition method
MLP	0.00	49.95	25.36	0.00	0.00	26.67	1
MLP	0.00	6.84	53.15	0.00	0.00	20.73	2
RBF	0.00	0.00	0.00	29.46	0.00	8.74	1
RBF	72.41	0.00	6.62	0.00	14.69	17.73	2
SVM	0.00	6.97	5.25	0.00	0.00	3.08	1
SVM	33.36	0.00	10.18	0.00	0.00	10.53	2

Table I-8(b1) Percent prediction accuracy for OHC loss using the three models.

Model \ Frequency	0.5kHz	1kHz	2kHz	4kHz	8kHz	Average	Partition method
MLP	94.93	78.48	83.88	95.03	90.27	88.52	1
MLP Band Based	94.93	86.46	90.25	95.03	91.40	91.61	1
MLP	87.19	82.50	80.00	93.75	85.63	85.81	2
MLP Band Based	89.06	82.50	83.44	93.75	89.69	87.69	2
RBF	96.37	90.99	95.44	93.79	86.25	92.69	1
RBF Band Based	96.37	90.99	95.44	94.73	87.99	93.11	1
RBF	96.25	87.50	94.69	94.38	82.19	91.00	2
RBF Band Based	96.25	90.00	94.69	97.19	85.94	92.81	2
SVM	95.03	90.48	92.86	91.00	88.51	91.57	1
SVM Band Based	96.37	92.65	92.86	93.90	89.44	93.04	1
SVM	92.81	89.69	90.00	94.69	90.31	91.50	2
SVM Band Based	95.94	89.69	90.00	96.25	90.31	92.44	2

Table I-8(b2) Improvement in the percent error rate for the prediction of OHC loss using the three models (Band based vs Overall).

Model \ Frequency	0.5kHz	1kHz	2kHz	4kHz	8kHz	Average	Partition method
MLP	0.00	37.08	39.52	0.00	11.61	26.92	1
MLP	14.60	0.00	17.20	0.00	28.25	13.25	2
RBF	0.00	0.00	0.00	15.14	12.65	5.75	1
RBF	0.00	20.00	0.00	50.00	21.06	20.11	2
SVM	26.96	22.79	0.00	32.22	8.09	17.44	1
SVM	43.53	0.00	0.00	29.38	0.00	11.06	2

Table I-8(c) Percent of prediction accuracy of PTS loss for three models.

Model \ Frequency	0.5kHz	1kHz	2kHz	4kHz	8kHz	Average	Partition method
MLP	91.00	94.61	88.61	94.20	92.14	92.11	1
MLP Band Based	94.82	95.74	88.61	94.20	92.24	93.12	1
MLP	89.38	95.00	80.94	91.88	90.00	89.44	2
MLP Band Based	93.44	95.00	83.13	94.06	91.25	91.38	2
RBF	95.65	95.34	94.31	96.17	89.54	94.20	1
RBF Band Based	95.65	95.44	95.27	96.17	90.17	94.53	1
RBF	96.25	92.81	92.50	96.88	82.81	92.25	2
RBF Band Based	96.25	92.81	92.50	96.88	89.69	93.63	2
SVM	93.99	95.55	88.10	93.07	91.82	92.51	1
SVM Band Based	94.10	96.28	89.34	93.48	92.03	93.05	1
SVM	95.00	98.13	87.19	91.88	88.75	92.19	2
SVM Band Based	95.00	98.13	90.31	92.19	91.88	93.50	2

Table I-8(c2) Improvement in the percent error rate for the prediction of PTS using the three models (Band based vs Overall).

Model \ Frequency	0.5kHz	1kHz	2kHz	4kHz	8kHz	Average	Partition method
MLP	42.44	20.96	0.00	0.00	1.27	12.80	1
MLP	38.23	0.00	11.49	26.85	12.50	18.37	2
RBF	0.00	2.15	16.87	0.00	6.02	5.69	1
RBF	0.00	0.00	0.00	0.00	40.02	17.81	2
SVM	1.83	16.40	10.42	5.92	2.57	7.21	1
SVM	0.00	0.00	24.36	3.82	27.82	16.77	2

Conclusion: It is not surprising that the band based approach can yield improved prediction models than by the overall method. The weakness of the band based selection is that the models are more complicated compared to the overall models.

(7) DPOAE results (177 animals)

Among the 322 animal data base, 177 animals were tested for DPOAE pre-, during and post-exposure. The DPOAE parameters were checked in three prediction models. The ATS is also considered as input variable to check its contribution for the prediction models with DPOAE variables. Table I-9 shows the input-output variables of the prediction models.

Table I-9: Inputs and outputs variables for complex noise.

Inputs (independent variables)	Outputs (dependent variables)
Noise metrics: 1. Weighted energy, $E_w(t)$; 2. Kurtosis in time domain, $\beta(t)$; 3. Probability of a transient occurring in impulse/impact noise, P; 4. Kurtosis in frequency domain $\beta(f)$ at cf = 1, 2, 4, 8 kHz; 5. Weighted energy in filtered octave bands $E_w(f)$ at cf = 1, 2, 4, 8 kHz; 6. The energy of background noise, $E_b(t)$; 7. Pre-exposure auditory evoked potential thresholds, $PRE_{EP}(f)$ at cf = 1, 2, 4, 8 kHz; 8. A threshold shift, $TS(f)$ at cf = 1, 2, 4, 8 kHz 9. Pre-exposure cubic distortion product otoacoustic emission, $PRE_{DPOAE}(f)$ at cf = 1, 2, 4, 8 kHz.	Indices of trauma to the auditory system (at specific center frequencies): 1. Noise-induced PTS, $PTS(f)$ (dB) at cf = 1, 2, 4, 8 kHz; 2. Outer hair cell loss, $OHC(f)$(%) at cf = 1, 2, 4, 8 kHz; 3. Inner hair cell loss, $IHC(f)$ (%)at cf = 1, 2, 4, 8 kHz; 4. Permanent change in DPOAE, $\Delta DPOAE(f)$ (dB) at cf = 1, 2, 4, 8 kHz.

Table I-9(a) Percent prediction accuracy for IHC loss using the three models.

Frequency / Model	1kHz	2kHz	4kHz	8kHz	Average	Partition method
MLP All	81.59	82.12	85.52	82.51	82.94	1
MLP no ATS	87.03	80.27	90.77	85.48	85.89	1
MLP no DPO	85.13	83.43	83.08	85.87	84.38	1
MLP no DPO & ATS	78.01	85.53	94.92	88.88	86.83	1
MLP All	84.66	88.64	86.93	75.00	83.81	2
MLP no ATS	88.64	84.09	84.09	75.00	82.95	2
MLP no DPO	89.77	87.50	84.66	87.50	87.36	2
MLP no D & ATS	100.00	92.05	81.25	88.07	90.34	2
RBF All	89.26	88.70	89.29	82.86	87.53	1
RBF no ATS	87.96	87.37	89.29	85.69	87.58	1
RBF no DPO	86.98	90.77	89.11	84.55	87.85	1
RBF no DPO & ATS	84.91	88.51	90.61	86.81	87.71	1
RBF All	86.36	87.50	88.64	84.66	86.79	2
RBF no ATS	88.64	90.34	86.93	90.91	89.20	2
RBF no DPO	86.93	87.50	88.07	82.39	86.22	2
RBF no DPO & ATS	89.77	94.89	86.36	93.18	91.05	2
SVM All	86.62	77.77	87.75	83.62	83.94	1
SVM no ATS	86.60	77.77	87.95	86.25	84.64	1
SVM no DPO	84.15	81.36	91.54	86.07	85.78	1
SVM no DPO & ATS	84.70	81.35	92.11	87.02	86.30	1
SVM All	85.80	73.86	88.64	82.95	82.81	2
SVM no ATS	85.23	75.00	89.20	83.52	83.24	2
SVM no DPO	75.57	78.98	92.05	88.64	83.81	2
SVM no DPO & ATS	88.64	77.84	88.64	89.77	86.22	2

Table I-9(a) shows percent prediction accuracy for IHC loss using the three models. There are four structures in each model. The performance of three models was similar on IHC loss prediction. Among the four structures the one without DPOAE and ATS inputs obtained the highest prediction accuracy, which means the DPOAE and ATS may be not necessary for IHC loss prediction models.

Table I-9(b) Percent of prediction accuracy of OHC loss for three models.

Frequency / Model	1kHz	2kHz	4kHz	8kHz	Average	Partition method
MLP All	78.76	76.09	73.85	82.85	77.89	1
MLP no ATS	67.23	70.32	85.69	79.68	75.73	1
MLP no DPO	80.24	65.53	84.80	80.63	77.80	1
MLP no DPO & ATS	83.66	83.96	87.58	83.83	84.76	1
MLP All	71.02	76.14	73.30	83.52	75.99	2
MLP no ATS	84.09	75.00	72.73	77.84	77.41	2
MLP no DPO	75.00	72.16	90.34	68.75	76.56	2
MLP no D & ATS	80.11	85.23	77.84	86.93	82.53	2
RBF All	83.98	86.07	86.84	82.65	84.88	1
RBF no ATS	83.43	86.65	87.97	85.11	85.79	1
RBF no DPO	85.68	88.70	90.43	84.16	87.24	1
RBF no DPO & ATS	85.13	89.45	93.06	86.25	88.47	1
RBF All	78.98	86.36	88.07	76.14	82.39	2
RBF no ATS	82.95	84.09	86.36	81.25	83.66	2
RBF no DPO	91.48	86.93	89.20	90.91	89.63	2
RBF no DPO & ATS	81.82	87.50	89.77	80.11	84.80	2
SVM All	81.71	76.52	80.08	80.96	79.81	1
SVM no ATS	83.03	77.44	84.02	82.09	81.65	1
SVM no DPO	85.29	81.76	84.80	84.34	84.05	1
SVM no DPO & ATS	85.30	85.51	87.80	84.56	85.79	1
SVM All	77.27	71.59	82.95	78.98	77.70	2
SVM no ATS	79.55	77.27	81.82	82.95	80.40	2
SVM no DPO	84.09	77.27	86.93	87.50	83.95	2
SVM no DPO & ATS	86.93	85.23	85.80	79.55	84.38	2

Table I-9(b) shows percent prediction accuracy for OHC loss using the three models. There are four structures for each model. The performance of the three models was similar at OHC loss prediction. Among the four structures the one without DPOAE and ATS inputs got the highest prediction accuracy, which means the DPOAE and ATS may be not necessary for OHC loss prediction model.

Table I-9(c) Percent of prediction accuracy of PTS loss for three models.

Frequency / Model	1kHz	2kHz	4kHz	8kHz	Average	Partition method
MLP All	86.29	78.55	71.77	83.98	80.15	1
MLP no ATS	84.79	88.18	83.42	81.78	84.54	1
MLP no DPO	84.55	77.98	83.28	83.80	82.40	1
MLP no DPO & ATS	89.31	82.13	93.22	85.53	87.55	1
MLP All	81.82	80.68	85.23	84.09	82.95	2
MLP no ATS	83.52	84.09	83.52	84.66	83.95	2
MLP no DPO	82.95	80.68	85.80	88.07	84.38	2
MLP no D & ATS	90.34	95.45	80.68	88.07	88.64	2
RBF All	89.29	89.67	90.58	85.70	88.81	1
RBF no ATS	87.07	87.80	90.21	85.13	87.55	1
RBF no DPO	89.47	92.10	93.03	87.39	90.50	1
RBF no DPO & ATS	87.99	92.12	92.47	87.95	90.13	1
RBF All	86.93	90.91	86.93	81.82	86.65	2
RBF no ATS	85.80	88.07	93.75	83.52	87.78	2
RBF no DPO	87.50	92.61	93.75	87.50	90.34	2
RBF no DPO & ATS	82.95	93.18	96.02	86.93	89.77	2
SVM All	83.27	84.02	84.36	84.74	84.10	1
SVM no ATS	87.41	80.83	89.63	86.83	86.18	1
SVM no DPO	84.97	84.22	85.48	86.06	85.18	1
SVM no DPO & ATS	90.80	83.64	89.44	87.95	87.96	1
SVM All	75.00	84.09	87.50	88.64	83.81	2
SVM no ATS	86.93	88.07	89.77	79.55	86.08	2
SVM no DPO	85.80	86.36	88.64	84.66	86.36	2
SVM no DPO & ATS	87.50	83.52	90.91	89.77	87.93	2

Table I-9(c) shows percent prediction accuracy for PTS using the three models. There are four structures for each model. The performance of the three models was similar at PTS prediction. Among the four structures the one without DPOAE and ATS inputs had the highest prediction accuracy, which means the DPOAE and ATS may be not necessary for PTS prediction model.

Table I-9(d) Percent of prediction accuracy of DPOAE loss for three models.

Frequency / Model	1kHz	2kHz	4kHz	8kHz	Average	Partition method
MLP All	81.70	83.59	80.98	80.03	81.58	1
MLP no ATS	83.62	90.58	84.77	86.05	86.26	1
MLP All	79.55	78.98	82.95	84.66	81.53	2
MLP no ATS	84.66	88.64	80.68	85.80	84.94	2
RBF All	87.94	92.84	90.21	88.14	89.78	1
RBF no ATS	87.02	92.28	90.60	88.33	89.56	1
RBF All	85.23	88.64	94.32	84.66	88.21	2
RBF no ATS	89.77	86.36	89.20	87.50	88.21	2
SVM All	84.74	81.91	79.89	86.45	83.25	1
SVM no ATS	84.18	80.82	80.64	86.84	83.12	1
SVM All	78.98	82.39	80.11	83.52	81.25	2
SVM no ATS	86.36	85.80	77.27	86.36	83.95	2

Table I-9(d) shows percent prediction accuracy for DPOAE loss using the three models. There are four structures for each model. The performance for three models was similar in the DPOAE loss prediction. The performance of the three models with or without ATS has no significantly difference (in the MLP model ATS input made the performance worse), thus ATS should not be used as an input in the DPOAE loss prediction model.

Conclusion: It seems that there is not strong relationship between pre-exposure DPOAE and NIHL, i.e. the DPOAE makes no contribution to the NIHL prediction model. This conclusion agrees with the results described in Davis, et al. (2004).

(8) Independent test of the prediction models

To test the performance of the proposed prediction models, a group of animals (Group 277) which was not used in the process of constructing the prediction models, was tested in each prediction model. Twelve animals in Group 277 were exposed to a complex noise environment having broadband (710~5680Hz) impulses and background Gaussian noise with SPL = 100 dB(A), $\beta(t) = 33$. Table 1-10(a) shows the average IHC loss prediction accuracy for three models based on 12 random training/test data runs, Table 1-10(b) the average OHC loss prediction accuracy and Table I-10(c) the average PTS prediction accuracy.

Table I-10(a) Percent prediction accuracy for IHC loss using different models (Group 277).

Frequency / Model	0.5kHz	1kHz	2kHz	4kHz	8kHz	Average	Partition method
MLP	100	100	92	83	100	95	1
MLP	100	100	100	100	100	100	2
RBF SF model	100	100	100	50	100	90	1
RBF WF model	100	100	100	83	100	82	2
SVM SF model	100	100	100	75	100	95	1
SVM WF model	100	100	100	25	100	85	2

Table I-13(b) Percent prediction accuracy for OHC loss using different models (Group 277).

Frequency / Model	0.5kHz	1kHz	2kHz	4kHz	8kHz	Average	Partition method
MLP	100	100	100	100	92	98	1
MLP	100	100	100	100	100	100	2
RBF SF model	100	100	83	58	92	87	1
RBF WF model	92	100	58	67	100	83	2
SVM SF model	100	100	100	50	92	88	1
SVM WF model	100	100	100	100	100	100	2

Table I-13(c) Percent prediction accuracy for PTS using different models (Group 277).

Frequency / Model	0.5kHz	1kHz	2kHz	4kHz	8kHz	Average	Partition method
MLP	100	100	100	100	42	92	1
MLP	100	75	100	100	100	95	2
RBF SF model	100	100	100	100	100	100	1
RBF WF model	100	100	100	83	83	93	2
SVM SF model	100	100	100	83	100	97	1
SVM WF model	100	100	100	67	100	93	2

Figures 1 through 18 illustrate the individual IHC loss, OHC loss and PTS evaluated using the three prediction models. Figures I-1 to I-3 show the estimations of IHC loss, OHC loss and PTS using MLP model with partition method 1. Figures I-4 to I-6 show the estimations using MPL model with partition method 2. Figures I-7 to I-9 display the estimation using RBF model with partition method 1, figures I-10 to I-12 with partition method2. Figures I-13 to I-18 illustrate the estimations from the SVM model with

partition 1 and 2. The circle and the bar in the figures are the mean OHC loss or IHC loss, or PTS and standard deviation of the test group respectively, while the asterisk (*) indicates the model's predicted values. All three prediction models provide a good estimated (within one standard deviation) of IHC, OHC loss and PTS.

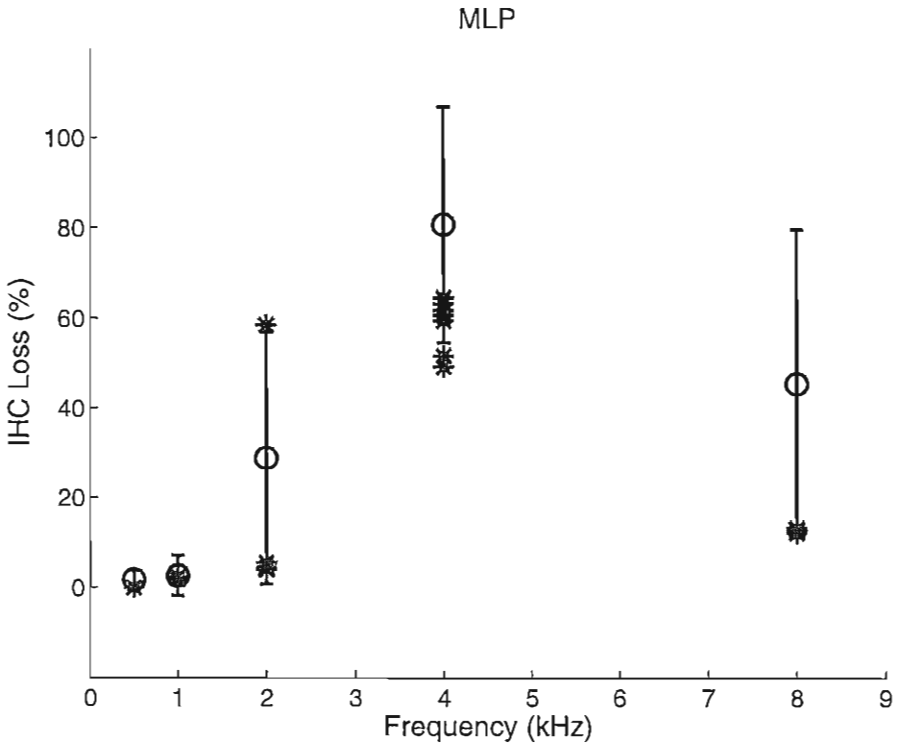

Figure I-1 Percent prediction accuracy for IHC loss using the MLP model (partition method 1).

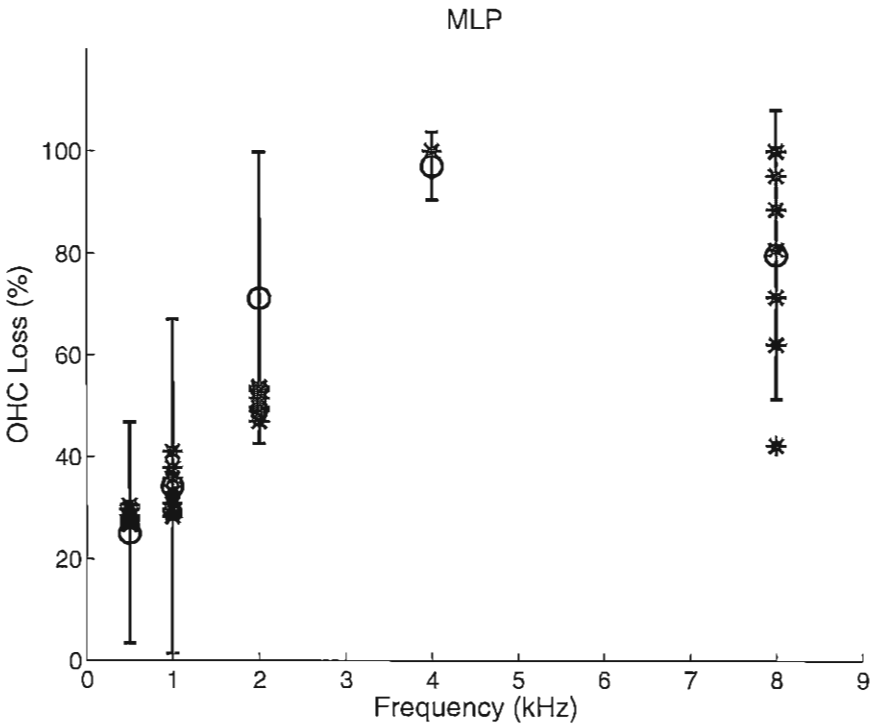

Figure I-2 Percent prediction accuracy for OHC loss the MLP model (partition method 1).

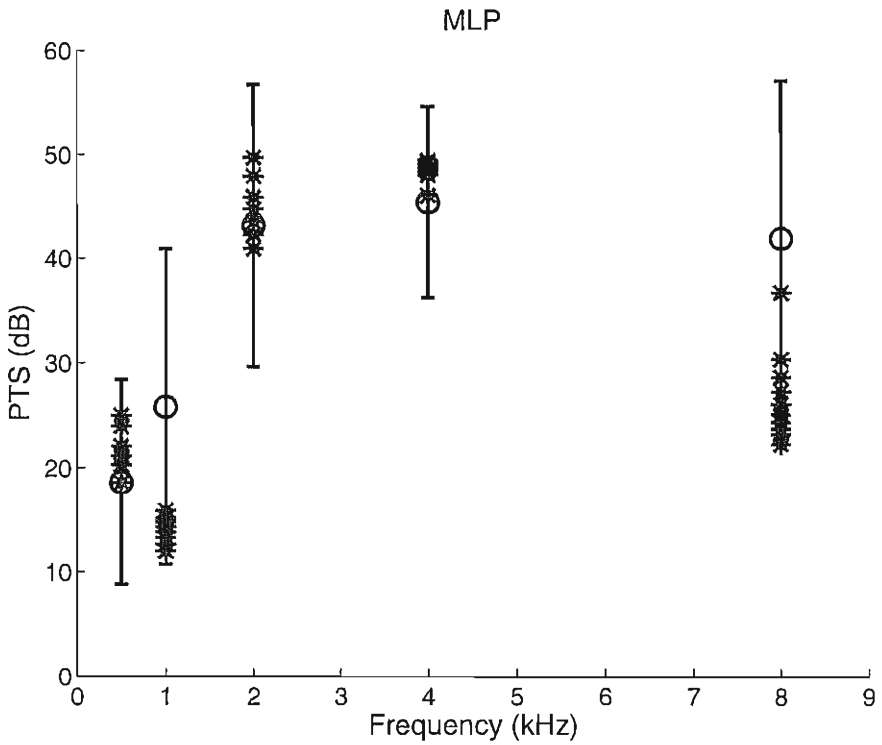

Figure I-3 Percent prediction accuracy for PTS using the MLP model (partition method 1).

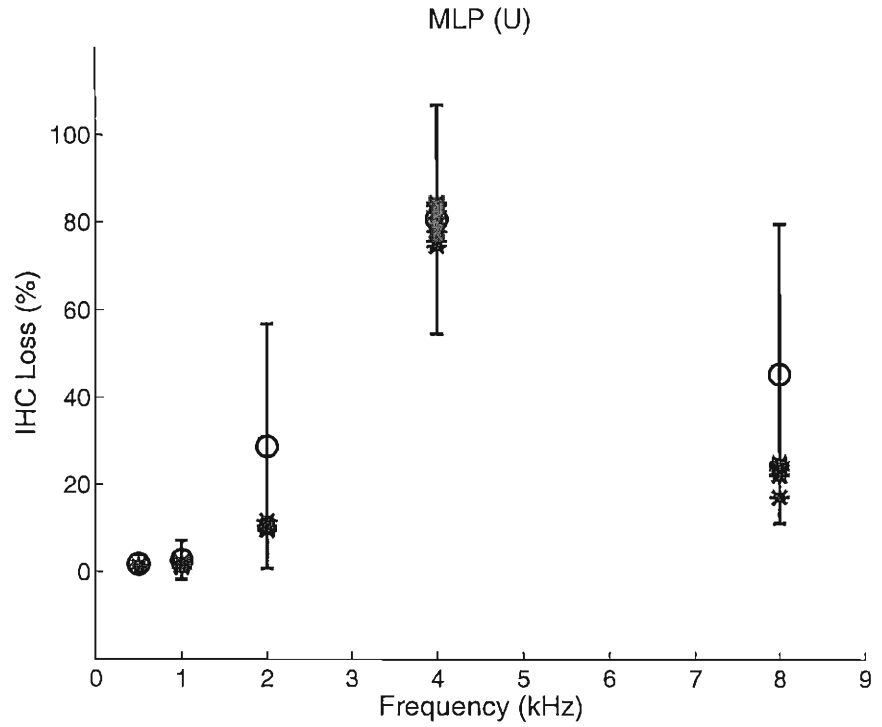

Figure I-4 Percent prediction accuracy for IHC loss using the MLP model (partition method 2)

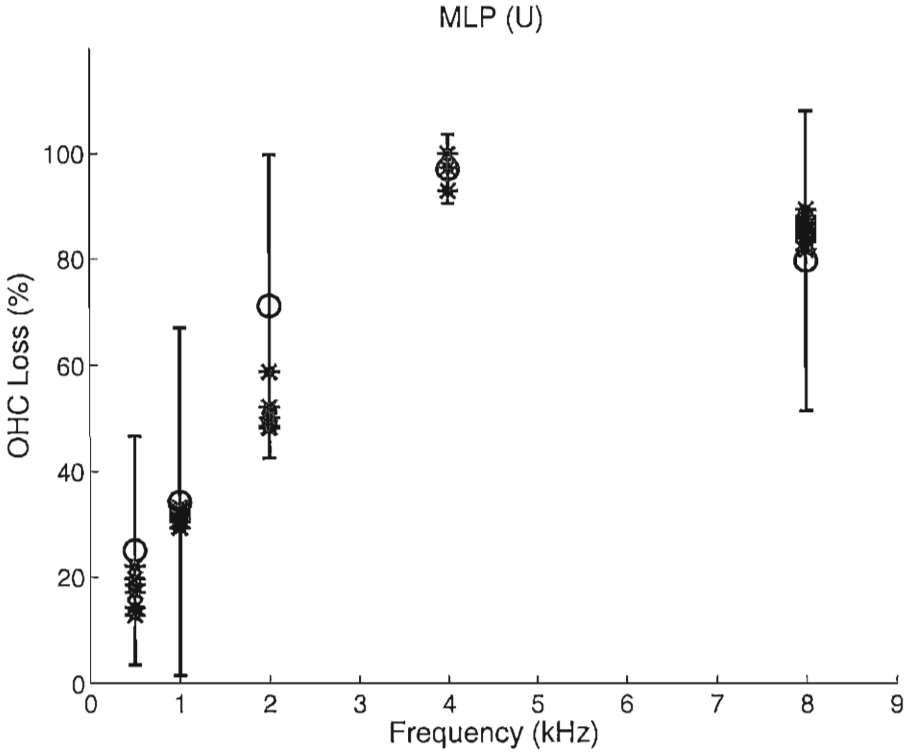

Figure I-5 Percent prediction accuracy for OHC loss using the MLP model (partition method 2).

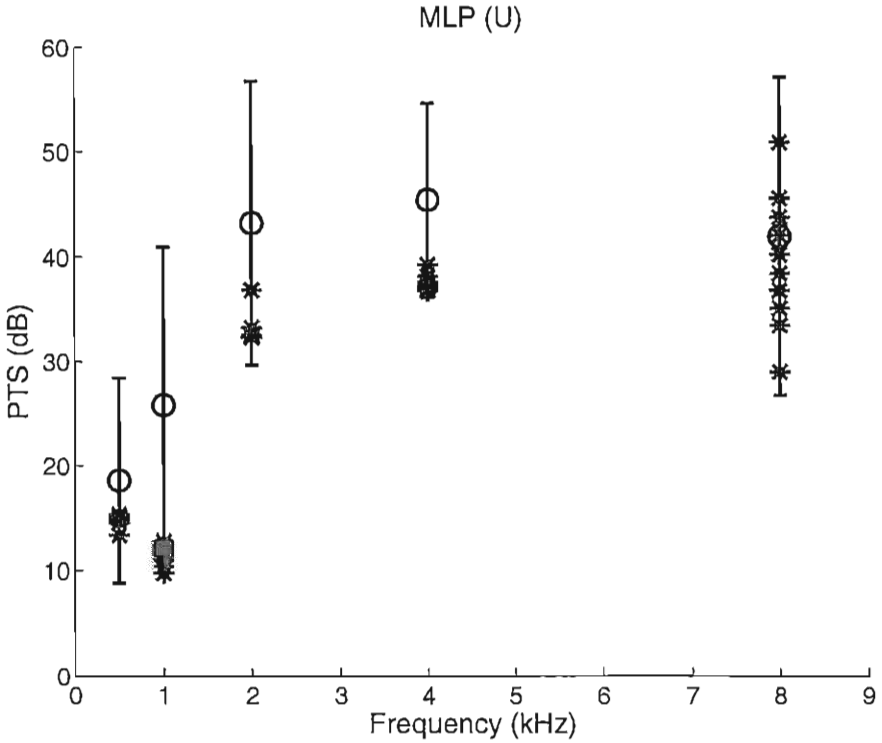

Figure I-6 Percent prediction accuracy for PTS using the MLP model (partition method 2).

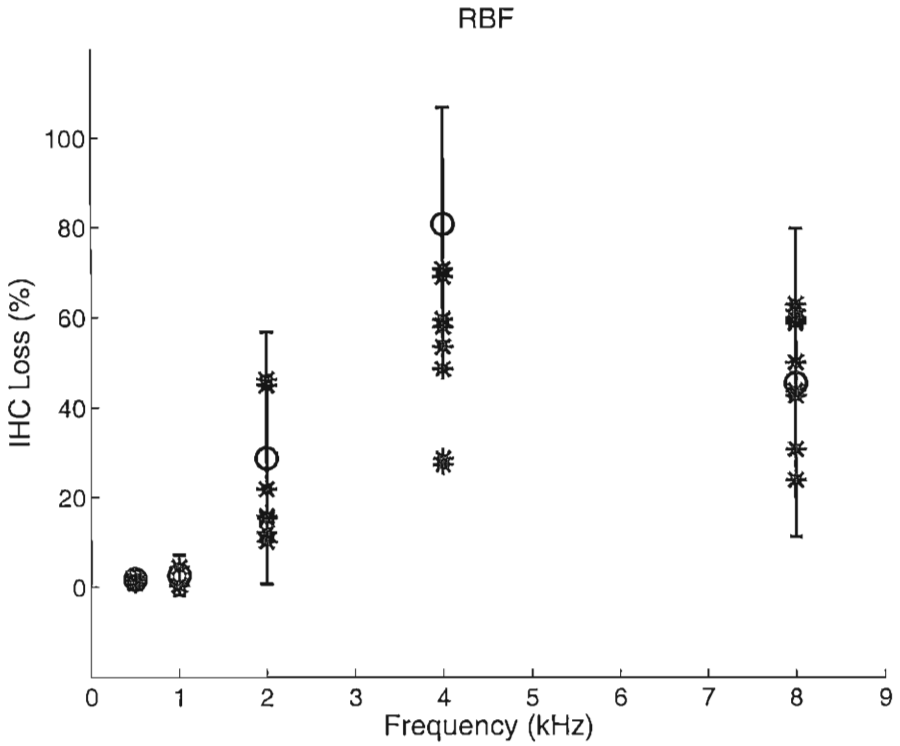

Figure I-7 Percent prediction accuracy for IHC loss using the RBF model (partition method 1)

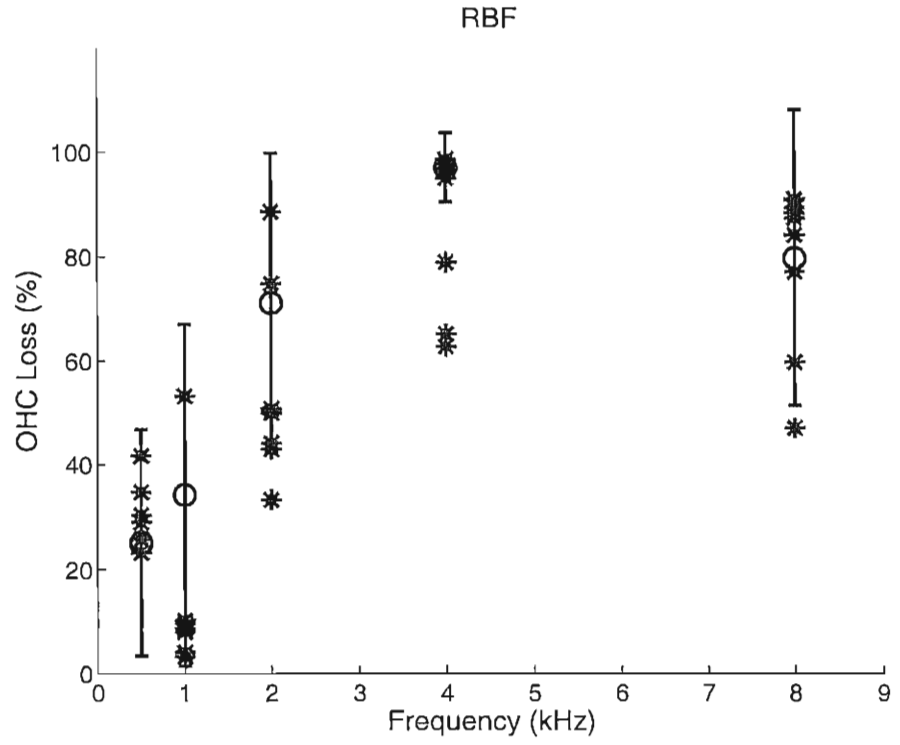

Figure I-8 Percent prediction accuracy for OHC loss using the RBF model (partition method 1).

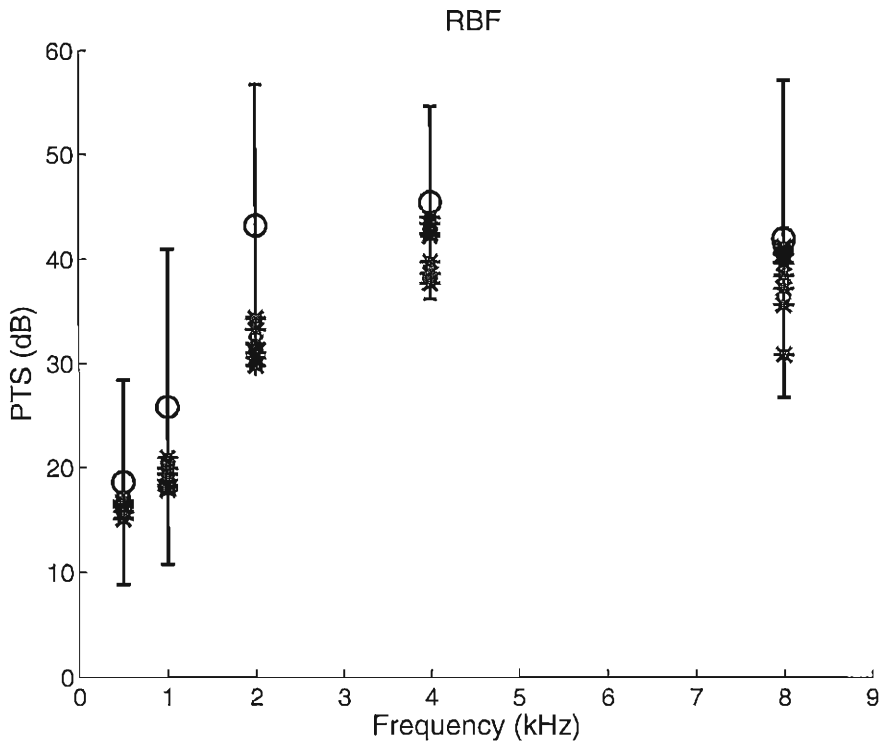

Figure I-9 Percent prediction accuracy for PTS using the RBF model (partition method 1).

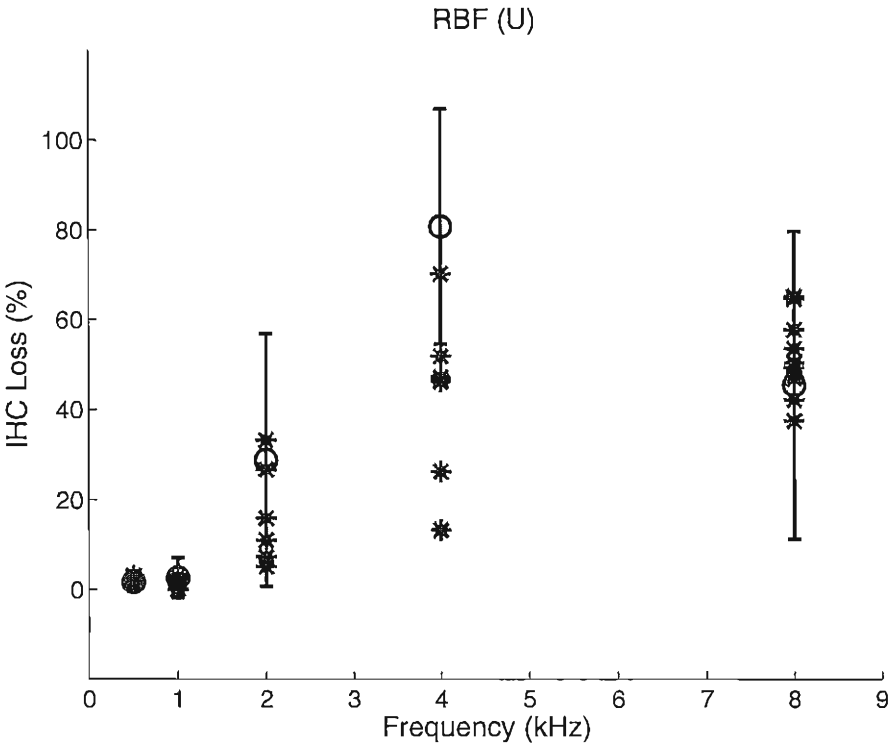

Figure I-10 Percent prediction accuracy for IHC loss using the RBF model (partition method 2).

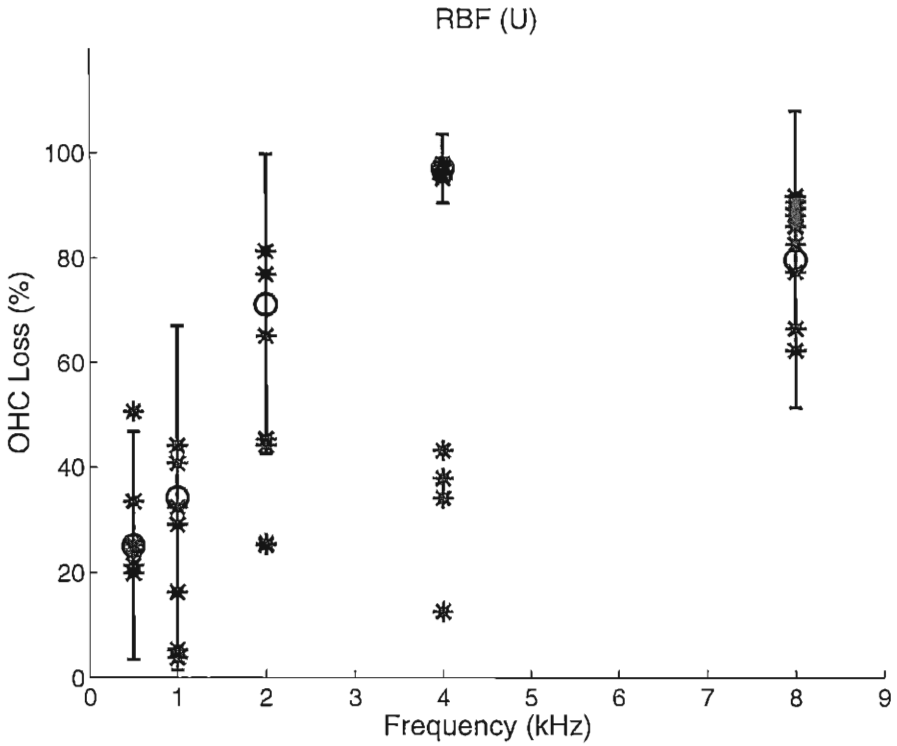

Figure I-11 Percent prediction accuracy for OHC loss using the RBF model (partition method 2).

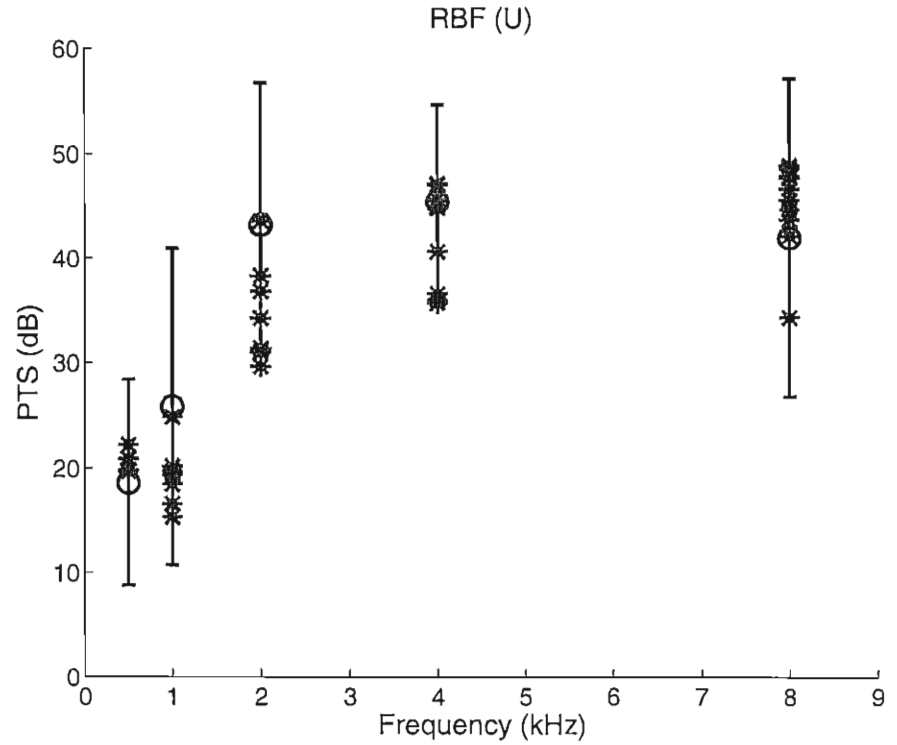

Figure I-12 Percent prediction accuracy for PTS using the RBF model (partition method 2)

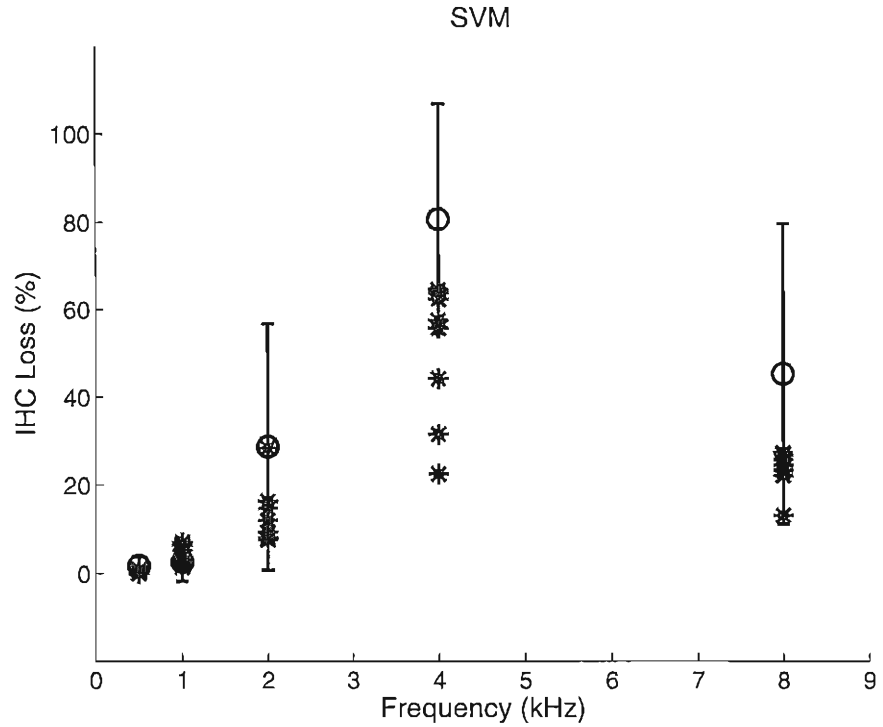

Figure I-13 Percent prediction accuracy for IHC loss using the SVM model (partition method 1).

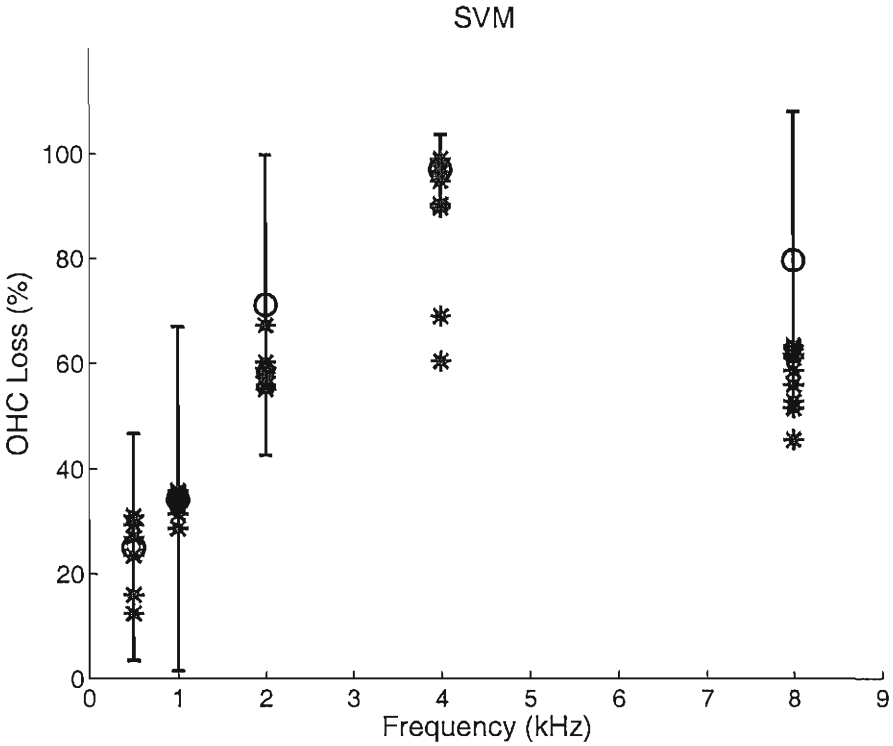

Figure I-14 Percent prediction accuracy for OHC loss using the SVM model (partition method 1)

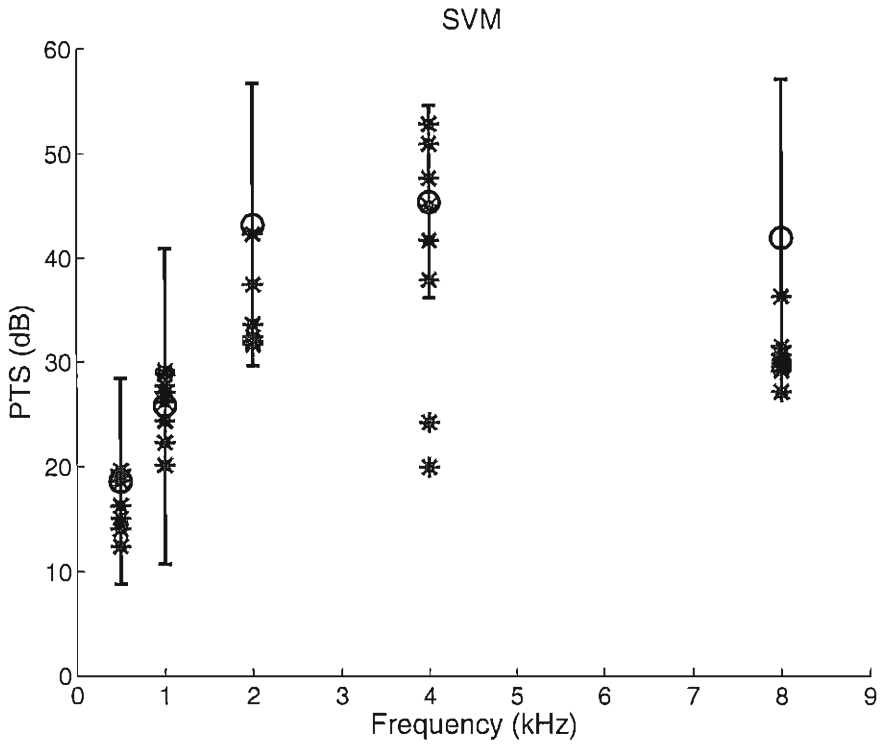

Figure I-15 Percent prediction accuracy for PTS using the SVM model (partition method 1).

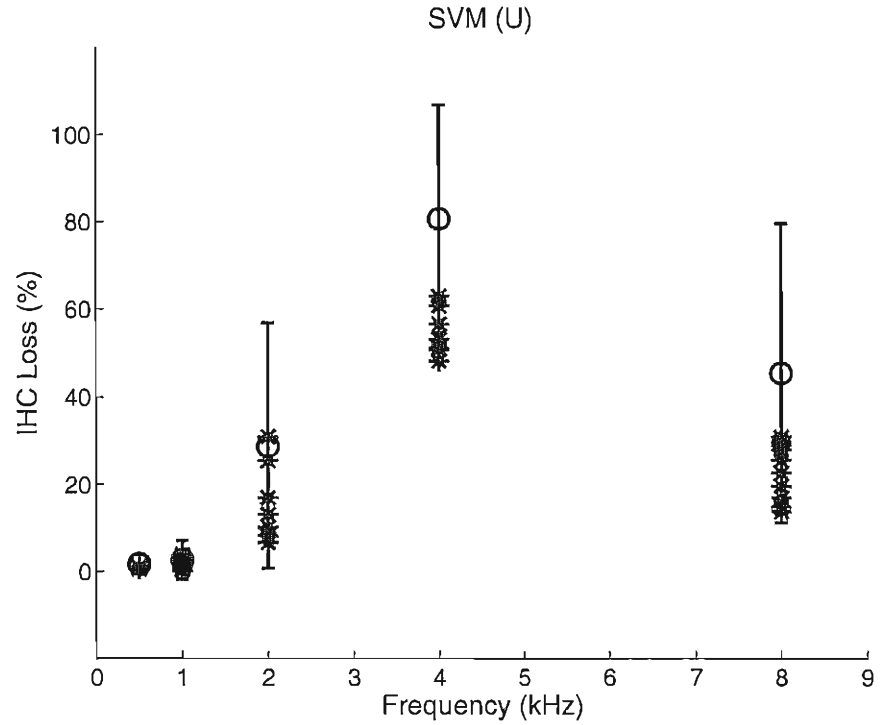

Figure I-16 Percent prediction accuracy for IHC loss using the SVM model (partition method 2).

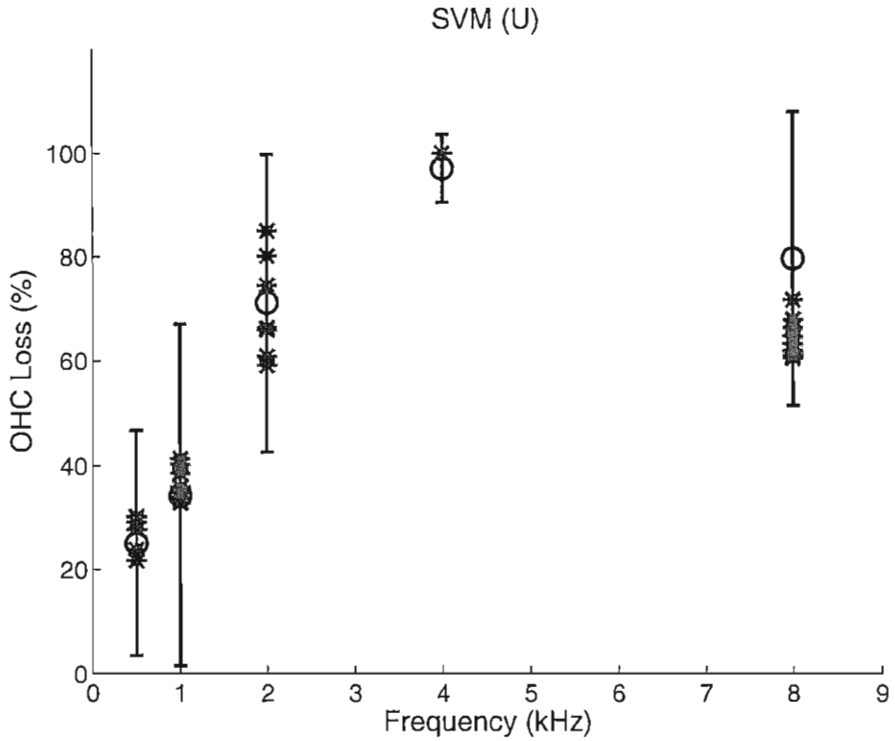

Figure I-17 Percent prediction accuracy for OHC loss using SVM (partition method 2).

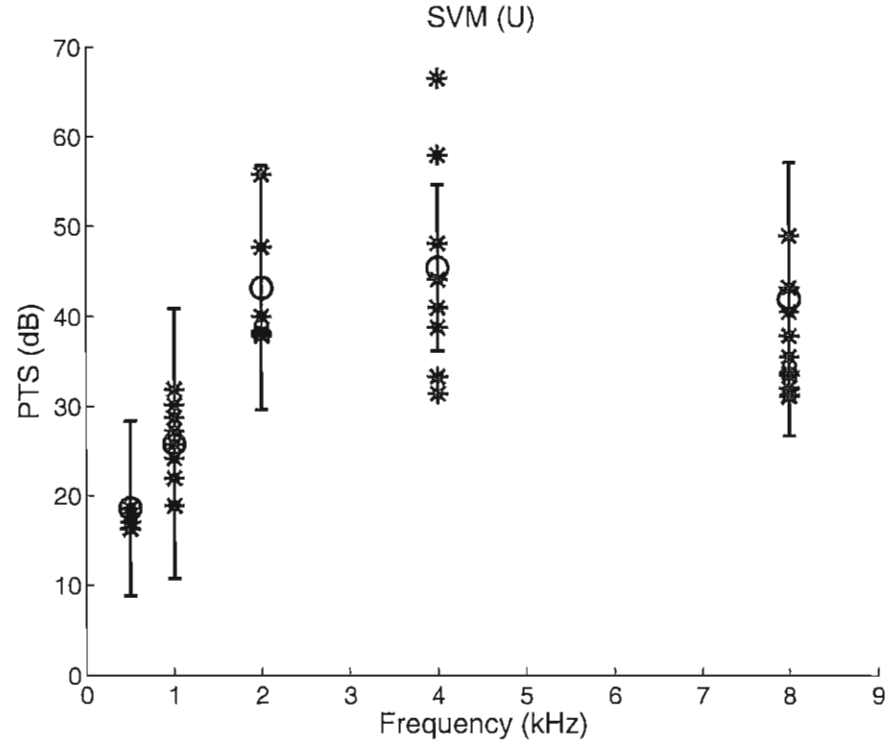

Figure I-18 Percent prediction accuracy for PTS using the SVM model (partition method 2)

Part II: Prediction models for high level impulse noise exposures

In the case of high level impulse/impact noises, two types of models were constructed and tested. One type is the specific frequency model (SF model), which is denoted as the 'SF model', and the other type is the both-side wide band frequency model (WF model), which is denoted as the 'WF model'. A total 578 animals were exposed to 151 to 160 dB peak SPL impulse noises. The input and output variables for the models are listed in Table II-1.

Table II-1 Input and output variables for high level impulse noise exposures.

Inputs (independent variables)	Outputs (dependent variables)
Noise metrics: 1. Weighted energy, $E_w(t)$; 2. Weighted energy in filtered octave bands $E_w(f)$ at cf = 0.5, 1, 2, 4, 8 kHz; 3. Impulse peak pressure, P_{peak}; 4. Impulse duration, D; 5. Impulse rate, R; 6. Impulse number, N; 7. Pre-exposure auditory evoked potential thresholds, $PRE_{EP}(f)$ at cf = 0.5, 1, 2, 4, 8 kHz;	Indices of trauma to the auditory system (at specific center frequencies): 1. Noise-induced PTS, $PTS(f)$ (dB) at cf = 0.5, 1, 2, 4, 8 kHz; 2. Outer hair cell loss, $OHC(f)$(%) at cf = 0.5, 1, 2, 4, 8 kHz; 3. Inner hair cell loss, $IHC(f)$ (%)at cf = 0.5, 1, 2, 4, 8 kHz;

Table II-1(a1) Percent prediction accuracy for IHC loss using the three models.

Frequency / Model	0.5kHz	1kHz	2kHz	4kHz	8kHz	Average	Partition method
MLP SF model	71.82	70.42	73.18	72.95	73.88	72.45	1
MLP WF model	75.61	72.21	73.65	78.26	70.25	73.99	1
MLP SF model	71.35	75.17	63.72	73.09	73.09	71.28	2
MLP WF model	69.97	71.53	72.92	71.18	71.70	71.46	2
RBF SF model	84.60	87.90	89.33	84.20	84.43	86.09	1
RBF WF model	86.39	85.24	85.76	84.49	82.64	84.90	1
RBF SF model	85.94	84.38	86.98	86.81	86.28	86.08	2
RBF WF model	84.38	84.38	85.94	85.59	80.90	84.24	2
SVM SF model	86.91	85.59	84.20	82.18	86.27	85.03	1
SVM WF model	87.37	82.88	80.63	85.06	84.20	84.03	1
SVM SF model	84.03	84.38	82.47	84.03	83.51	83.68	2
SVM WF model	87.33	78.13	82.47	84.90	81.08	82.78	2

Table II-2(a2) Change of prediction error rate for IHC loss using the three models (WF vs SF).

Frequency / Model	0.5kHz	1kHz	2kHz	4kHz	8kHz	Average	Partition method
MLP	13.45	6.05	1.75	19.63	-13.90	5.59	1
MLP	-4.82	-14.66	25.36	-7.10	-5.17	0.63	2
RBF	11.62	-21.98	-33.46	1.84	-11.50	-8.55	1
RBF	-11.10	0.00	-7.99	-9.25	-39.21	-13.22	2
SVM	3.51	-18.81	-22.59	16.16	-15.08	-6.68	1
SVM	20.66	-40.01	0.00	5.45	-14.74	-5.51	2

Table II-1(a1) presents the percent prediction accuracy for IHC loss using SF and WF methods. Table II-1(a2) shows the improvement in prediction error rate in comparison the WF to the SF. The performance of the RBF and SVM models was very close (around 85% prediction accuracy), while the MLP model is more than 10% lower than that of the RBF and SVM models. The SF method in RBF and SVM model was better than that of the WF method. Although in the MLP model using the WF seems a little bit better than the SF method, the overall accuracy of MLP was much lower than other two models. Thus in IHC loss prediction models the SF approach should be used.

Table II-1(b1) Percent prediction accuracy for OHC loss using the three models.

Frequency / Model	0.5kHz	1kHz	2kHz	4kHz	8kHz	Average	Partition method
MLP SF model	73.04	80.58	73.53	63.86	75.72	73.34	1
MLP WF model	80.73	77.81	74.05	71.00	71.97	75.11	1
MLP SF model	77.95	83.16	71.01	70.31	59.20	72.33	2
MLP WF model	78.65	80.56	75.52	69.62	78.99	76.67	2
RBF SF model	82.58	87.20	90.49	83.21	87.60	86.22	1
RBF WF model	86.73	85.87	83.39	85.58	86.45	85.60	1
RBF SF model	81.77	86.11	88.89	80.73	88.72	85.24	2
RBF WF model	86.46	82.47	83.68	85.76	87.85	85.24	2
SVM SF model	88.18	88.70	86.97	81.95	86.45	86.45	1
SVM WF model	88.01	86.91	82.99	80.69	85.47	84.81	1
SVM SF model	85.94	90.97	86.81	84.55	85.94	86.84	2
SVM WF model	88.72	84.72	83.16	79.34	80.90	83.37	2

Table II-2(b2) Change of prediction error rate for OHC loss using the three models (WF vs SF).

Frequency / Model	0.5kHz	1kHz	2kHz	4kHz	8kHz	Average	Partition method
MLP	28.52	-14.26	1.96	19.76	-15.44	6.64	1
MLP	3.17	-15.44	15.56	-2.32	48.50	15.68	2
RBF	23.82	-10.39	-74.66	14.12	-9.27	-4.50	1
RBF	25.73	-26.21	-46.89	26.10	-7.71	0.00	2
SVM	-1.44	-15.84	-30.54	-6.98	-7.23	-12.10	1
SVM	19.77	-69.21	-27.67	-33.72	-35.85	-26.37	2

Table II-1(b1) presents the percent prediction accuracy for OHC loss using SF and WF methods. Table II-1(b2) shows change of prediction error rate in comparison the WF to the SF. The performance of the RBF and SVM models was very close (around 85% prediction accuracy), while the MLP model was around 10% lower than that of the RBF and SVM models. The RBF and SVM models with the SF method were better than that of the WF method. Although in the MLP model using the WF seems a little bit better than the SF, the overall accuracy of the MLP is much lower than other two models. Thus in OHC loss prediction model the SF approach should be used.

Table II-1(c1) Percent prediction accuracy for PTS using the three models.

Model \ Frequency	0.5kHz	1kHz	2kHz	4kHz	8kHz	Average	Partition method
MLP SF model	87.83	89.62	87.94	91.23	86.34	88.59	1
MLP WF model	89.05	87.27	92.50	89.05	86.63	88.90	1
MLP SF model	92.01	88.37	96.35	83.51	81.77	88.40	2
MLP WF model	89.76	89.24	89.24	86.98	90.28	89.10	2
RBF SF model	87.49	93.02	92.33	89.50	91.87	90.84	1
RBF WF model	90.02	88.93	88.58	90.37	91.70	89.92	1
RBF SF model	89.58	90.28	91.67	88.89	90.63	90.21	2
RBF WF model	88.19	88.37	85.24	87.85	88.72	87.67	2
SVM SF model	91.82	93.25	93.31	91.92	93.89	92.84	1
SVM WF model	93.08	92.15	92.16	92.62	93.66	92.73	1
SVM SF model	92.36	92.36	93.06	94.44	92.36	92.92	2
SVM WF model	91.49	88.72	89.06	91.32	91.63	90.24	2

Table II-2(c2) Change of prediction error rate for PTS using the three methods (WF vs SF).

Model \ Frequency	0.5kHz	1kHz	2kHz	4kHz	8kHz	Average	Partition method
MLP	10.02	-22.64	37.81	-24.86	2.12	2.72	1
MLP	-28.16	7.48	-194.79	21.04	46.68	6.03	2
RBF	20.22	-58.60	-48.89	8.29	-2.09	-10.04	1
RBF	-13.34	-19.65	-77.19	-9.36	-20.38	-25.94	2
SVM	15.40	-16.30	-17.19	8.66	-3.76	-1.54	1
SVM	-11.39	-47.64	-57.64	-56.12	-9.55	-37.85	2

Table II-1(c1) presents the percent prediction accuracy for PTS using the three models with the SF and WF methods. Table II-1(c2) shows change of the prediction error rate in comparison the WF to the SF. The performance of the SVM model was the best in PTS prediction (more than 90%), while performance of the RBF and MLP was close. The RBF and SVM models with SF method were obviously better than that of the WF method, and in the MLP model using the WF seems a little bit better than that of using the SF. In the PTS prediction models the use of the SF approach is suggested.

Conclusion: For high level impulse noise environments, exposure parameters, i.e. peak, duration, number and rate, are important to the prediction of NIHL. The SVM and RBF models using the SF method obtained as much as 90% prediction accuracy. The overall performance of SVM model using the SF is a little bit better than that of the RFB model. The SVM model using the SF method was selected as the final prediction model for high level impulse noise exposures.

Part III. **Selecting the final prediction model**

A model with the minimum error rate R was selected as the final prediction model. Figure III-1 gives a diagrammatic summary of the best model selection procedure.

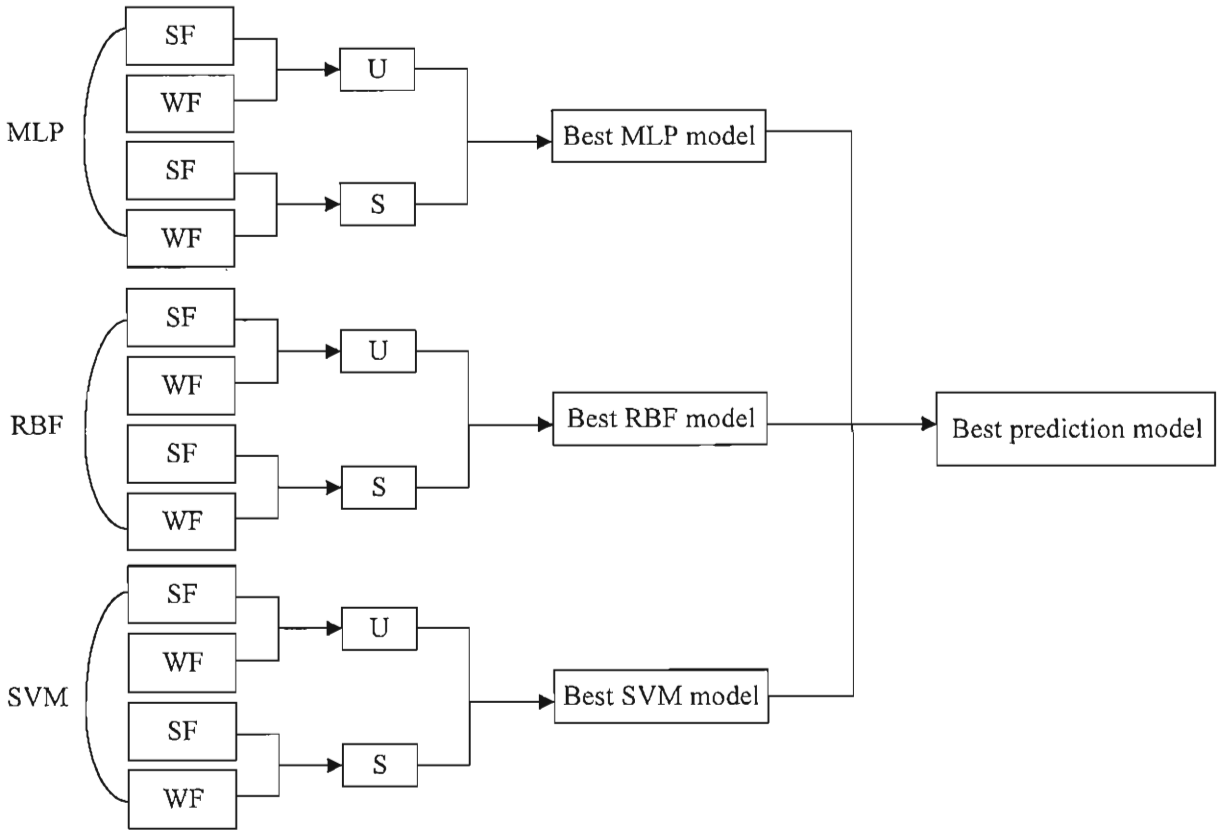

Figure III-1 A diagrammatic description of the best prediction model selection. [Note: SF: Specific frequency prediction model; WF: Wide band frequency prediction model; U: Universal model; S: Specific model (see page 7).

(A) Best prediction model for low and medium level (peak<140dB) complex long term noise exposures (Gaussian or non-Gaussian):

The RBF prediction model with the upper-side WF method was selected as the best prediction model for NIHL from complex long term noise (Gaussian or non-Gaussian). The input and output variables are listed in Table III-1.

Table III-1 Input and output variables of the RBF prediction model for complex long term noise exposure.

Inputs (independent variables)	Outputs (dependent variables)
Noise metrics: 1. Weighted energy, $E_w(t)$; 2. Kurtosis in time domain, $\beta(t)$; 3. Probability of a transient occurring in impulse/impact noise, *Prob*; 4. Kurtosis in frequency domain $\beta(f)$ at cf = 0.5, 1, 2, 4, 8 kHz; 5. Weighted energy in filtered octave bands $E_w(f)$ at cf = 0.5, 1, 2, 4, 8 kHz; 6. The energy of background noise, $E_b(t)$; 7. Pre-exposure auditory evoked potential thresholds, $PRE_{EP}(f)$ at cf = 0.5, 1, 2, 4, 8 kHz;	Indices of trauma to the auditory system (at specific center frequencies): 1. Noise-induced PTS, *PTS(f)* (dB) at cf = 0.5, 1, 2, 4, 8 kHz; 2. Outer hair cell loss, *OHC(f)*(%) at cf = 0.5, 1, 2, 4, 8 kHz; 3. Inner hair cell loss, *IHC(f)* (%)at cf = 0.5, 1, 2, 4, 8 kHz;

(B) Best prediction model for high peak level (peak>140dB) impulse noise transients with short duration:

The SVM prediction model with the SF method was selected as the best prediction model for NIHL from high level impulse noise transients with short duration. The input and output variables are listed in Table III-2

Table III-2 Input and output variables of the RBF prediction model for high level impulse noise exposure.

Inputs (independent variables)	Outputs (dependent variables)
Noise metrics: 1. Weighted energy, $E_w(t)$; 2. Weighted energy in filtered octave bands $E_w(f)$ at cf = 0.5, 1, 2, 4, 8 kHz; 3. Impulse peak pressure, P_{peak}; 4. Impulse duration, *D*; 5. Impulse rate, *R*; 6. Impulse number, *N*; 7. Pre-exposure auditory evoked potential thresholds, $PRE_{EP}(f)$ at cf = 0.5, 1, 2, 4, 8 kHz;	Indices of trauma to the auditory system (at specific center frequencies): 1. Noise-induced PTS, *PTS(f)* (dB) at cf = 0.5, 1, 2, 4, 8 kHz; 2. Outer hair cell loss, *OHC(f)*(%) at cf = 0.5, 1, 2, 4, 8 kHz; 3. Inner hair cell loss, *IHC(f)* (%)at cf = 0.5, 1, 2, 4, 8 kHz;

Publications:

1. Qiu, W., Ye, J., Liu-White, X.H., and Hamernik, R.P. (2005). Model for noise-induced hearing loss using support vector machine. *J. Acoust. Soc.Am.* 118(3), Pt. 2: 1896.
2. Qiu, W.,Chang, C.Q., Liu, W.Q., Poon, P.W.F., Hu, Y., Lam, F.K., Hamernik, R.P., Wei, G., and Chan, F.H.Y. (2006). Real-time data-reusing adaptive learning of a radial basis function network for tracking evoked potentials, IEEE Trans. on Biomedical Eng., 53(2): 226-237.
3. Qiu, W., Ye, J., and Hamernik, R.P. (2006). The development of models for the prediction of noise-induced hearing loss, *4th Joint Meeting ASA and ASJ, Honolulu, Hawaii* (submitted).
4. Qiu, W., Ye, J., and Hamernik, R.P. (2006). The application of statistical learning models to the prediction of noise-induced hearing loss, *4th Joint Meeting ASA and ASJ, Honolulu, Hawaii* (submitted)

Literature Cited.

Bies, D.A. and Hansen, C.H. (1990) An alternative mathematical description of the relationship between noise exposure and hearing loss. *J. Acoust. Soc. Am.* 88:2743-2754.

Bies, D.A. (1994). An alternative model for combining noise and age-induced hearing loss. J. Acoust. Soc. Am. 95:563-565.

Bishop, C.M. (1995) *Neural networks for pattern recognition*, Oxford: Clarendon Press.

Brownell, W.E., Bader, C.R., Bertand, D., and de Ribauierre, Y. (1985) Evoked mechanical response of isolated cochlear hair cells, *Science*, 227:194-196.

Cherkassky, V and Mulier, F. (1998) *Learning from data, concepts, theory, and methods*. John Wiley & Sons, Inc., New York.

Chinrungrueng, C. and Sequin, C.H. (1995) Optimal adaptive *k*-means algorithm with dynamic adjustment of learning rate, *IEEE Trans. Neural Networks*, vol. 6, pp. 157-169

Criosi, F. and Poggio, T. (1990) Networks and the best approximation property. Biological Cybernetics. 63:169-176.

Cybenko, G. (1989) Approximation by superpositions of a sigmoidal function. *Mathematics of Control, Signal, and System.* 2:304:314.

Davis, B., Qiu, W., and Hamernik, P.R. (2004). The use of distortion product otoacoustic emissions in the estimation of hearing and sensory cell loss in noise-damaged cochleas, *Hearing Research*, 187: 12-24.

Dayhoff, J.E. (1990) *Neural Network Architectures, An Introduction*. Van Nostrand Reinhold, New York, NY.

Demuth, H. and Beale, M. (2000) *Neural network toolbox for use with Matlab*, The MathWork, Inc.

Dobie, R.A. (1993) *Medical-Legal Evaluation of Hearing Loss*. Van Nostrand Reinhold, New York.

Eldredge, D.H., Miller, J.D. and Bohne, B.A. (1981) A frequency-position map for the chinchilla cochlea. *J. Acoust. Soc. Am.*, 69:1091-1095.

Erdreich, J. (1986) A distribution based definition of impulse noise, *J. Acoust. Soc. Am.* 79:990-998.

Geman, S., Bienenstock, E. and Doursat, R. (1992) Neural networks and the bias/variance dilemma, *Neural Computation*, 4(1):1-58.

Hagan, M.T., Demuth H.B. and Beale M. (1996) *Neural network design*, PWS Publishing Company, Boston, MA.

Hamernik, R.P., Patterson, J.H., Turrentine, G.A., and Ahroon, W.A. (1989) The quantitative relation between sensory cell loss and hearing thresholds, *Hear. Res.*, 38:199-211.

Hamernik, R.P., Ahroon, W.A. Davis R.I., Lei S-F (1994) Hearing threshold shifts from repeated 6-h daily expsure to impact noise. *J. Acoust. Soc. Am.* 95:444-453.

Hamernik, R.P., Ahroon, W.P., Lei, S-F. (1996) The cubic distortion product otoacoustic emissions from the normal and noise-damaged chinchilla cochlea. J. Acoust. Soc. Am. 100:1003-1012.

Hamernik, R.P. and Ahroon, W.A. (1998) Interrupted noise exposure: threshold shift dynamics and permanent effects, *J. Acoust. Soc. Am.* 103(6):3478-3488.

Hamernik, R.P. and Qiu, W. (2001) Energy-independent factors influencing noise-induced hearing loss in the chinchilla model, *J. Acoust. Soc. Am.,* 110(6):3163-3168.

Hamernik, R.P., Ahroon, W.A., Patterson, J.H. and Qiu, W. (2002) Relations among early postexposure noise-induced threshold shifts and permanent threshold shifts in the chinchilla, *J. Acoust. Soc. Am.* 111(1):320-326.

Hamernik, R.P, Qiu, W. and Davis B. (2003) The effects of the amplitude distribution of equal energy exposures on noise-induced hearing loss: The kurtosis metric. *J. Acoust. Soc. Am.* 114(1): 386-395.

Hartman, E. J., Keeler J. D. and Kowalski J. M. (1990) Layered neural networks with Gaussian hidden units as universal approximations. *Neural Computation* 2(2): 210-215.

Haykin, S. (1999) *Neural networks: A Comprehensive Foundation*, Macmillian College Publishing Company, New York.

Hornik, K. M., Stinchcombe M. and White H. (1989). Multilayer feedforword networks are universal approximators. *Neural Networks*, 2(5): 359-366.

Humes, L.E. and Jesteadt, W. (1991). Modeling the interactions between noise exposure and other variables, J. Acoust. Soc. Am. 90, 182-188.

Hush, D.R., and Horne, B.G. (1993) Progress in supervised neural networks: What's new since Lippmann? *IEEE Signal Processing Magazine*, 10:8-39.

International Organization for Standardization (1990). *Acoustics: Determination of Occupational Noise Exposure and Estimation of Noise-Induced Hearing Impairment, ISO-1999.* Geneva: International Organization for Standardization.

Johnson D.L. (1994) The development of the data base for ISO-1999, an evaluation of its strengths and weaknesses. *J. Acoust. Soc. Am.* (A) 95; 2861.

Kecman, V. (2001) *Learning and soft computing, support vector machines, neural network, and fuzzy logic models*. The MIT Press, Cambridge, Massachusetts.

Kraak, W. (1981) Investigations on criteria for the risk of hearing loss due to noise, In: Tobias, J.V. and Schubert, E.D. Eds. Hearing research and theory, Volume I, New York: Academic Press, 187-303.

Kryter, K.D. (1970) Evaluation of exposure to impulse noise, *Arch. Environ. Health* 20:624-635.

Kurkova, V. (1992) Kolmogorov's theorem and multilayer neural network, *Neural Networks* 5:501-506.

Lei, S.-F., Ahroon, W.A., and Hamernik, R.P. (1994) The Application of Frequency and Time Domain Kurtosis to the Assessment of Hazardous Noise Exposures. *J. Acoust. Soc. Am.* 96:3:1435-1444.

Lei, S.-F. and Hamernik, R.P. (1998). Construction of a joint peak-interval histogram using higher-order cumulant based inverse filtering. 1998 International Conference on Acoustics, Speech and Signal Processing, Seattle, WA, May 12-15.

Liberman, M.C. and Dodds, L.W. (1984) Single-neuron labeling and chronic cochlear pathology, II: Stereocilia damage and alterations in threshold tuning curves, *Hear. Res.*, 16:55-74.

Macrae, J.H. (1991). Presbycusis and noise-induced permanent threshold shift. J. Acoust. Soc. Am. 90:2513-2516.

Mills, J.H., Osguthorpe, J.D., Burdick, C.K., Patterson, J.H., Jr., and Mozo, B. (1983) Temporary threshold shifts produced by exposure to low-frequency noises, *J. Acoust. Sco. Am.* 73:918-923.

Mills, J.H., Lee F.S., Dubno, J.R. and Boettcher, F.A. (1996) Interactions between age-related and noise-induced hearing loss, In: Axelsson, A., Borchrevink, H., Hamernik, R.P., Hellstrom, P.-A., Henderson, D. and Salvi, R.J. Eds. Scientific basis noise-induced hearing loss, New York: Thieme Medical Publishers, Inc., 1996:193-212.

Mills, J.H., Boettcher, F.A., and Dubno, J.R. (1997). Interaction of noise-induced permanent threshold shift and age-related threshold shift, J. Acoust. Soc. Am. 101, 1681-1686.

Nelson, D.A. and Kiester, T.E. (1978). Frequency discrimination in the chinchilla. *J. Acoust. Soc. Am.* 64: 114-126.

Nguyen, D., and Widrow, B. (1990). Improving the learning speed of 2-layer neural networks by choosing initial values of the adaptive weights, *Proceedings of the International Joint Conference on Neural Networks*, Vol. 3, 21-26.

NORA (1996): National Occupational Research Agenda, U.S. Department of Health and Human Services.

Park, J. and Sandberg, I. W. (1991) Universal approximation using radial basis function networks, *Neural Computation* 3(2): 246-257.

Patterson, M.H. Jr., Hamernik, R.P. (1992) An experimental basis for the estimation of auditory system hazard following exposure to impulse noise, In: Dancer, A.L, Henderson, D., Salvi, R.J. and Hamernik, R.P. Eds. Noise-Induced Hearing Loss, New York: Mosby-Year Book, Inc., 1992:336-348.

Patterson J.H.Jr., Hamernik, R.P., Hargett, C.E., and Ahroon, W.A. (1993) An isohazard function for impulse noise, J. Acoust. Soc. Am. 93(5):2860-2869.

Price, G.R. (1983) Relative hazard of weapons impulses. *J. Acoust. Soc. Am.* 73:556-566.

Price, G.R. and Kalb, J.T. (1991) Insights into hazard from intense impulses from a mathematical model of the ear. *J. Acoust. Soc. Am.* 90:219-227.

Reger, S.N. and Lierle, D. (1954) Changes in auditory acuity produced by low and medium intensity-level exposures, *J. Acoust. Soc. Am.*, 58:433-438.

Scales, L. E. (1985) *Introduction to non-linear optimization*, Springer-Verlag, New York.

Smith, M. (1993) *Neural networks for statistical modeling*, New York: Van Nostrand Reinhold.

Suykens, J.A.K., Gestel, T.V., Brabanter, J.D., Moor, B.D. and Vandewalle, J. (2002) *Least Squares Support vector Machines*, New Jersey: World Scientific.

Vapnik, V.N. (1995) *The Nature of Statistical Learning Theory*, New York: Springer Verlag.

Ward, W.D. (1991) The role of intermittence in PTS, *J. Acoust. Soc. Am.* 90:164-169.

Ward, W.D. (1994), Z24-X-2 forty years later. *J. Acoust. Soc. Am.* (A) 95; 2860.

Widrow, B. and Hoff, M.E. (1960) Adaptive switching circuits, *IRE WESCON Convention Record*, New York: IRE Part 4: 96-104.